EXPERIMENTAL INVESTIGATIONS OF VISCOUS REMANENT MAGNETIZATION USING A CONTINUOUS MEASUREMENT SYSTEM

by

Maurice A. Tivey

Submitted in partial fulfillment of the

requirements of Bachelor of Science Degree with Honours

at

Dalhousie University

Halifax, Nova Scotia

March, 1979

DEPARTMENT OF GEOLOGY
DALHOUSIE UNIVERSITY
HALIFAX, NOVA SCOTIA
CANADA
B3H 4J1

DALHOUSIE UNIVERSITY, DEPARTMENT OF GEOLOGY

B.Sc. HONOURS THESIS

Author: Maurice A. Tivey

Title: Experimental Investigations of Viscous Remanent Magnetization using a Continuous Measurement System

Signature of author

Date: March 16, 1979

Distribution License

DalSpace requires agreement to this non-exclusive distribution license before your item can appear on DalSpace.

NON-EXCLUSIVE DISTRIBUTION LICENSE

You (the author(s) or copyright owner) grant to Dalhousie University the non-exclusive right to reproduce and distribute your submission worldwide in any medium.

You agree that Dalhousie University may, without changing the content, reformat the submission for the purpose of preservation.

You also agree that Dalhousie University may keep more than one copy of this submission for purposes of security, back-up and preservation.

You agree that the submission is your original work, and that you have the right to grant the rights contained in this license. You also agree that your submission does not, to the best of your knowledge, infringe upon anyone's copyright.

If the submission contains material for which you do not hold copyright, you agree that you have obtained the unrestricted permission of the copyright owner to grant Dalhousie University the rights required by this license, and that such third-party owned material is clearly identified and acknowledged within the text or content of the submission.

If the submission is based upon work that has been sponsored or supported by an agency or organization other than Dalhousie University, you assert that you have fulfilled any right of review or other obligations required by such contract or agreement.

Dalhousie University will clearly identify your name(s) as the author(s) or owner(s) of the submission, and will not make any alteration to the content of the files that you have submitted.

If you have questions regarding this license please contact the repository manager at dalspace@dal.ca.

Grant the distribution license by signing and dating below.

_____ _____

Name of signatory Date

TABLE OF CONTENTS

Abstract

This study showed that with a simple circuit modification this new continuous measurement system of viscous remanent magnetization (VRM) can be made more flexible as far as the magnitude of the applied field and VRM response are concerned. It also became evident that samples ought to be allowed to decay in a zero field for 24 hrs. prior to experimentation. The IRDP rocks showed two types of VRM behaviour i) a linear logt relationship ii) a linear logt relationship but with a distinct increase in slope at about 2×10^4 secs. Why this occurs is not clear, it may be due to experimental conditions or more likely due to some physical property of the rock. The Bermudan rocks in general showed no relationship with time, but this is probably due to their past experimental history. The determination of susceptibility using this apparatus is relatively quick and produced precise results. However care must be taken with rocks that acquire a viscous moment rapidly i.e. large viscosity coefficients.

Acknowledgements

I would like to thank my thesis advisor Dr. J. Hall for providing encouragement, inspiration and critical advice. I would also like to thank Charles Walls for his technical help and Dianne Crouse for typing this manuscript.

Purpose

The purpose of this study was to cover the four objectives outlined below:

1) To test the recently acquired continuous measurement viscous remanent magnetization (VRM) equipment. To find its good and bad points and possibly find ways to improve the system.

2) To test for viscous remanent magnetization in rocks from the Iceland Research Drilling Project (IRDP) and to see if the usually assumed logt relationship is obeyed (where t is the acquisition or decay time).

3) To test the logt relationship of certain Bermudan rocks and to compare with previous work done on them (Rice, 1978).

4) To determine the susceptibility of the samples tested above by using the VRM equipment. A potentially fast and accurate method?

Introduction

Viscous remanent magnetization (VRM) refers to the part of rock magnetism that is produced through the application of an external magnetic field for a period of time at a constant temperature (Trukhin, 1966).

Ewing (1885) proposed the name magnetic viscosity after observing the viscous magnetization of iron. Early experimental work was carried out by Mitkevich in the 1930's (see Sholpo, 1967 for a review). Preisach (1935) is noted for inventing the Preisach diagram, which is useful for analysing viscous and hysteretic processes and for attributing magnetic viscosity to the thermal activation of domain walls (Dunlop, 1973c). Thellier showed in 1937 that magnetic viscosity could play an important role in the formation of the natural remanent moment of rocks. Since then many theoretical and experimental studies into magnetic viscosity have been conducted (Street and Wooley, 1949; Street et al., 1952; Thellier, 1937, Barbier, 1951, 1953; Creer, 1957; Shimizu, 1960; Neel, 1950 and LeBorgne, 1960). In recent years most work on VRM has been focussed on lunar rocks (Dunlop, 1973c, Sholpo, 1967 for review) and oceanic rocks (Dunlop and Hale, 1976; Lowrie, 1974; Lowrie and Kent, 1978).

The Significance of Viscous Remanent Magnetization

Why are people interested in viscous magnetism? Basically there are at least four reasons for this interest (Sholpo, 1967). First of all viscous magnetism complicates paleomagnetic research by distorting the direction of primary magnetization. Secondly we would like to determine the nature of time stability of all other types of remanent magnetization since this stability is dependent on viscous processes. Thirdly as magnetite is the common magnetic mineral in rocks, viscous remanence would be of interest for the theory of ferromagnetism. Finally rocks of lunar origin which have been brought back to earth show the influence of the Earth's geomagnetic field as a viscous moment (Dunlop, 1973c).

Theories of VRM Aquisition

The Richter Model

Richter in 1937 first produced a quantitative theory of viscous magnetism, explaining the viscosity effects observed over a time scale of 0.01 to 1.0 seconds in 'soft' (low coercivity) iron (Dunlop, 1973c). Later, these effects were proved to be due to carbon diffusion rather than thermal activation (Dunlop, 1973c).

All the theories based on the thermal activation of magnetic viscosity start with the following equation (Dunlop, 1973c):

$$(1) \qquad \frac{dm}{dt} = n^{+} \frac{dP^{+}}{dt} \Delta m - n^{-} \frac{dP^{-}}{dt} \Delta m$$

with

$$(2) \qquad \frac{dP^{\pm}}{dt} = C \exp - \frac{E^{\pm}}{kT} = \frac{1}{\tau^{\pm}}$$

where

m = net magnetic moment

$n^{\pm}$ = the number of possibilities at time t of an increment of $\pm\Delta m$ in m i.e. by domain wall movement or rotation

$p^{\pm}$ = the probability of positive or negative increments

C = rate constant ($\simeq 10^{10}\ s^{-1}$)

k = Boltzmann's constant

T = absolute temperature

$E^{\pm}$ = the energy barriers of positive and negative domain wall movements

$\tau^{\pm}$ = constants becoming relaxation times for positive and negative incremental changes in m when $P^{\pm}$ is independent of m.

Richter envisions two physical models; one in which there are n single domain (SD) particles with two possible minimum energy states per particle with the moments being $\pm vJ_s$ (where v is volume and J_s is the spontaneous magnetisation). The other model has n independent domain walls in the same or different multidomain (MD) particle. In this case VRM is controlled by the activation of each wall over simple potential barriers next to their equilibrium positions. Only small wall displacements are possible because all the walls must cross the first barrier before any wall can cross the second barrier. $P^{\pm}$ is made independent of m so that $\tau^{\pm}$ become relaxation constants; this is true for both models

From these two models one finds that $m = (n^- - n^+)\ \Delta m/2$ with $n^- + n^+ = n$ integrating equation (1) gives a relaxation equation:

$$(3) \qquad m(t,\tau) = m_{eq} - (m_{eq} - m_o)\ \exp\ (-t/\tau)$$

where

$$(4) \qquad 1/\tau = (1/\tau^{+}) + (1/\tau^{-})$$

$m_o \equiv m(o,\tau)$ initial value

m_{eq} = the equilibrium value towards which m relaxes as $t \gg \tau$

This relaxation equation (3) describes the transition between the initial magnetization state, $m = m_o$ and the equilibrium state, $m = m_{eq}$. Richter then assumed a distribution haw (5) for a group of SD particles or domain walls; he chose a logarithmic function (6) although it is not immediately obvious why.

$$(5) \qquad n(\tau)d\tau = Nf(\tau)d\tau \qquad \text{with n = no. of particles or walls.}$$

$$(6) \qquad f(\tau)d\tau = \frac{1}{\log(\tau_2/\tau_1)} \cdot \frac{1}{\tau}\, d\tau$$

Combining equations (5) and (6) then combining this with equation (3) we can produce an expression for the VRM acquired in time t_a, in a field H, after being initially demagnetized ($m_o = o$).

$$(7) \qquad m_v(t_a,H) = \frac{Nm_{eq}(H)}{\log(\tau_2/\tau_1)} \int_{\tau_1}^{\tau_2} (1 - e^{-t_a/\tau}) \frac{1}{\tau}\, d\tau$$

where

N = total no. of particles or walls.

The solutions to equation (7) are:

$$m_v(t_a,H) = \frac{Nm_{eq}(H)}{\log(\tau_2/\tau_1)} \quad \frac{1}{\tau_1} - \frac{1}{\tau_2} \quad t_a \qquad t_a \ll \tau_1$$

$$m_v(t_a,H) = \frac{Nm_{eq}(H)}{\log(\tau_2/\tau_1)} \quad \log t_a - \log\tau_1 + C_1 \qquad \tau_1 \ll t_a \ll \tau_2$$

$$mv(t_a,H) = Nm_{eq}(H) \quad 1 - \frac{\tau}{\log(\tau_2/\tau_1)} \cdot \frac{e^{-t_a/\tau_2}}{t_a} \qquad t_a \gg \tau_2$$

A similar procedure can be followed to obtain the decay of VRM. The coefficients of viscosity for acquisition, Sa and decay, Sd can be shown to be numerically equal (Dunlop, 1973c).

Néel (1949) approximated Richter's theory by using the 'unblocking' of magnetization at $t = \tau$, as the thermoremanent theories (TRM) do. Hence equation (3) can be replaced by:

(9) $m(t,\tau) = m_o \quad (t<\tau)$ blocked state

$m(t,\tau) = m_{eq} \quad (t>\tau)$ unblocked/equilibrium state.

Basically Richter assumes that all the relaxation times contribute to the magnetization at any instant (Dunlop, 1973c). However Néel (1949) approximates this by assuming only one particle or wall contributes to the VRM at a time t. Néels model simplifies Richter's approach and allows certain dependencies to be shown, e.g.

1) VRM dependence on H

2) $f(\log\tau)$ = constant (i.e.) does not imply a uniform distribution of all the particle properties

3) IRM separate from VRM (IRM is the Isothermal remanent magnetization)

4) Differences in acquisition and decay coefficients

The Néel Viscosity Field Theory

The Richter approach to the theory of VRM work well for SD particles and MD symmetrical barriers, however it breaks down when MD assymmetrical barriers are introduced. Néel used unequal coercive forces a and b acting for positive and negative field induced magnetization changes. He used the Preisach diagram to work out the magnetization processes involved in viscous remanent magnetization. From Néel (1950, 1955) the VRM can be written as:

$$(10) \qquad J_v(t_a,H) + J_i(H) = P/2\ (H + S_v(\log t_a - \log t_o))^2$$

where the VRM is measured at time t_o after H is removed in which time there is decay. P is a constant derived from Rayleigh's coefficient. When $\log(t_a/t_o) \ll H/S_v$ (10) reduces to

$$(11) \qquad J_v(t_a,H) + J_i(H) = pS_vH(\log t_a - \log t_o) + (P/s)H^2$$

where the second term on the right is the induced magnetization, $J_i(H)$.

Several important features are predicted by Néel's viscosity field theory (1950, 1955). These are:

1) Logarithmic dependence of VRM on t_a (acquisition time)

2) Non-logarithmic decay of VRM for large applied fields (H) or small t_a, becoming logarithmic

3) $S_a = -S_d$ for 2)

4) An extended tail on the decay curve ($t_d >> t_a$)

5) VRM is proportional to H for small fields.

The Stacey Demagnetizing Field Theory

One drawback of Néel's theory (1950) was that the self-demagnetization effect of MD grains was assumed to be constant. Néel made some corrections to this in his 1955 theory. However, Stacey (1963) incorporates this effect into his theory of VRM in large MD grains. If we have a model of n identical walls in a single MD grain whose cross-section A is constant along its length. Any one jump or domain wall movement changes H_d (demagnetizing field) of the grain changing the energy barriers of all the other walls in the grain (Dunlop, 1973c). By looking at just one grain we can ensure all walls to have the same change in transition probabilities.

Assuming closely spaced barriers a wall at locations x_o has simultaneous possibilities of being activated to $x_o+\lambda$ or $x_o-\lambda$, where λ is an increment of x (Dunlop, 1973c). Whichever one occurs the activation energies ($E^{\pm}$) changes for all walls (including the wall at x_o) by a fixed amount. However n^+ and n^- do not change since the wall that jumped has the same probability of further positive (i.e.

$x_o+\lambda$ to $x_o+2\lambda$) or negative jumps as all the other walls (Dunlop, 1973c). From here Stacey (1963) used equation (1) where $n^+=n^-=n$. From this he arrived at equation (12):

$$(12) \qquad J_v(t_a,T) = \frac{H}{N} + \frac{kT}{A\lambda J_s N}(Q^* + \log t_a)$$

where

H/N is the induced magnetization

$kT/A\lambda J_s N$ is S_a the viscosity coefficient

Q^* is a variable dependent on particle properties A, λ and H_c (the microscopic coercive force).

Stacey's theory predicts the temperature dependence of the viscosity coefficients but falsely predicts an independence of H.

Previous Experimental Work

Viscous acquisition

A number of experiments have been performed under a large variety of conditions and on a wide range of materials and rocks. In general the VRM was observed to increase as the logarithm of aquisition time, t_a, but there are exceptions where non-linear effects were observed (Creer, 1970; Lowrie, 1974; Lowrie and Kent, 1978).

$dJ_v/dlogt_a$ has been reported to be constant for MD grains in sedimentary rocks (Briden, 1965), for (1-500 μm) sized magnetic grains (Shimizu, 1960) and for massive magnetite ore (Pechnikov, 1967 and Yakubailik, 1968). It has also been verified that this relation holds for SD materials such as alnico (Street and Wooley, 1949), red sediments containing hematite (Creer, 1957) and soils containing hematite and magnetite (LeBorqne, 1960).

Sometimes another relation, $d(J_v)^{1/2}/dlogt_a$, which can be derived from Néel's theory (1950) has also been demonstrated to be constant. However it is an approximation to the $dJ_v/dlogt_a$ relationship which is probably more fundamental than the $d(J_v)^{1/2}/dlogt_a$ law, because $dJ_v/dlogt_a$ has been observed over a much longer time than $d(J_v)^{1/2}/dlogt_a$ (Dunlop, 1973c).

The linear dependence of VRM on log t_a is the general observation, however non-linear dependence has been observed on a number of

occasions e.g. for volcanic rocks (Rimbert, 1959), for basalts (Creer, 1970; Lowrie, 1974). Creer (1970) observed an abrupt increase in the viscosity coefficient after a time of 10^3 to 10^4 seconds. Dunlop (1973c) attributes the non-linear behaviour (the changes in viscosity coefficient) due to the irregular grain distribution since this previously had been assumed to be uniform (Richter, 1937; Néel, 1950) (i.e. a normal distribution).

Viscous decay

Viscous decay like viscous acquisition has been the subject of numerous experiments (Barbier, 1951, 1953; Shimizu, 1960; Trukhin, 1966, Creer, 1957). Generally J_v decreases as the logarithm of decay time, t_d. Two types of decay can be recognised (Dunlop, 1973c).

1) $dJ_v/d\log t_d$ remains constant, $t_d >> t_a$ e.g. Shimizu, 1960
2) $dJ_v/d\log t_d$ is constant only when $t_d < t_a$ decreasing to zero for larger t_d e.g. Trukhin, 1966.

In general SD material shows type 2 decay and MD material has type 1 decay. Both SD and MD materials will show type 2 decay for very small applied fields (H) and type 1 decay for very large H.

Most authors have shown that the acquisition coefficient S_a is numerically equal to the decay coefficient, S_d determined from the initial slope of the decay curve (Barbier, 1951, 1953; Creer, 1957; Trukhin, 1966; LeBorgne, 1960).

Field dependence of viscosity coefficients

Most authors agree that in the Rayleigh region (i.e. small fields 0-10 oe) S_a and S_d are proportional to field, H (Creer, 1957; LeBorgne, 1960; Shimizu, 1960; Sholpo, 1967). There is also general agreement that S becomes independent of H in moderate fields (i.e. 50 oe). The viscosity coefficients obtained from $d(J_v)^{1/2}/d\log t_a$ are not the same as S_a and S_d which are obtained from $d(J_v)/d\log t_a$. It has been shown that $(J_v)^{1/2}$ plots are independent of field whereas (J_v) plots are field dependent (Sholpo, 1967).

Temperature dependence of viscosity coefficients

Both the Stacey (1963) and Neel (1950, 1955) theories predict the temperature dependence of S_a. Some experiments over broad temperature ranges show that $S_a \propto T$ except near the Curie point where S_a increases rapidly with T (Street and Wooley, 1949, Shimizu, 1960). Some experiments have shown wide variations in S with a small temperature increase above room temperature (Kawai and Kume, 1953; Trukhim, 1966). These variations may be a reflection of the inhomogeneity of the blocking temperature spectrum (Dunlop, 1973c).

Demagnetization and stability of VRM

Thermal demagnetization by heating affects those particles carrying VRM with the lowest relaxation times τ and stabilizes the

remaining VRM against room temperature decay for times less than the maximum τ affected by the heating (Dunlop, 1973c) i.e. after heating $S_d \simeq 0$ until a long enough time when S_d returns to its pre-heating value. Thermal demagnetization is a very efficient way of erasing VRM. Alternating field demagnetization seems to erase most of the VRM components since low af coercivities usually correspond to low τ leading to a decrease in S (Dunlop, 1973c). VRM acquired by igneous rocks can be erased by 300-400 oe fields (Biquand and Prévot, 1971) whereas limestones need fields of 900 oe to erase less than 50% of the VRM. This hardness is attributed to very fine hematite particles in the limestone which have a high coercivity ($H_{co\ 1st} \simeq$ 5000-10000oc, $H_{co\ magnetite} \simeq$ 3000 oe) (Biquand and Prévot, 1971).

Experimental Work

A total of 48 experimental VRM runs were conducted totalling 1054 hours from December 1978 to February 1979 inclusive. The bulk of the samples studied were from the Iceland Research Drill Project (IRDP). One sample was from a Nova Scotian diabase dyke (Davison, 1979) and the remainder were from a drill site in Bermuda.

The IRDP rocks were from basalt flows and dykes from the top 1 km of the hole, (i.e.) from between 1.5 and 2.5 km below the original surface of the lava pile, the Bermudan samples were oceanic submarine basalts.

All the IRDP rocks used had been initially demagnetized although they had been allowed to stand in the Earth's magnetic field before being tested. The past history of the Bermudan rocks was not as clear but they had been through electrical conductivity tests and allowed to remain in the Earth's field for at least a year.

Most samples were run with a 0.1 oe or 1.0 oe applied field, some were run using a0.5 or 0.2 oe field. After acquiring remanence for a certain period three samples were also run as decay experiments, so that the relationship between acquisition and decay could be analysed.

Before the results can be examined the equipment used to gather the data will be described.

Description of Equipment

The continuous measurement VRM system used in this study consists basically of four pieces of equipment.

i) Magnetometer and sensor - At the heart of the VRM system is a susceptibility/viscosity magnetometer (model SVM-1), made by the Schonstedt Instrument Company of Reston, Virginia. This magnetometer is connected to a fluxgate sensor coil which is placed inside a magnetic shield (S-66), see Figure 1. The sensor unit has a square cavity in it surrounded by coils, this is where the magnetic field is measured.

The magnetometer measures the field inside the cavity and indicates the field strength in emu on a digital display. There is a range of sensitivities, x1, $x10^{-1}$, $x10^{-2}$, $x10^{-3}$, $x10^{-4}$, in emu's (electromagnetic units). The sensor coil produces a magnetic field inside the sample cavity. The strength of this applied field varies from 0.1 oe in 0.1 oe steps to 1.0 oe. The output of the magnetometer is connected to an XY recorder.

ii) XY recorder - The magnetometer output is connected to the Y terminals of a Hewlett Packard XY recorder model 7035b (see Figure 1). The recorder makes a permanent record of the change in magnetization of the sample. The x-axis is connected to a wave generator (see iii) which provides the time base so that the change in magnetization (VRM) can be plotted against time. The XY recorder has a range of sensitivities for the X and Y axes, ranging from 10 volts/inch to

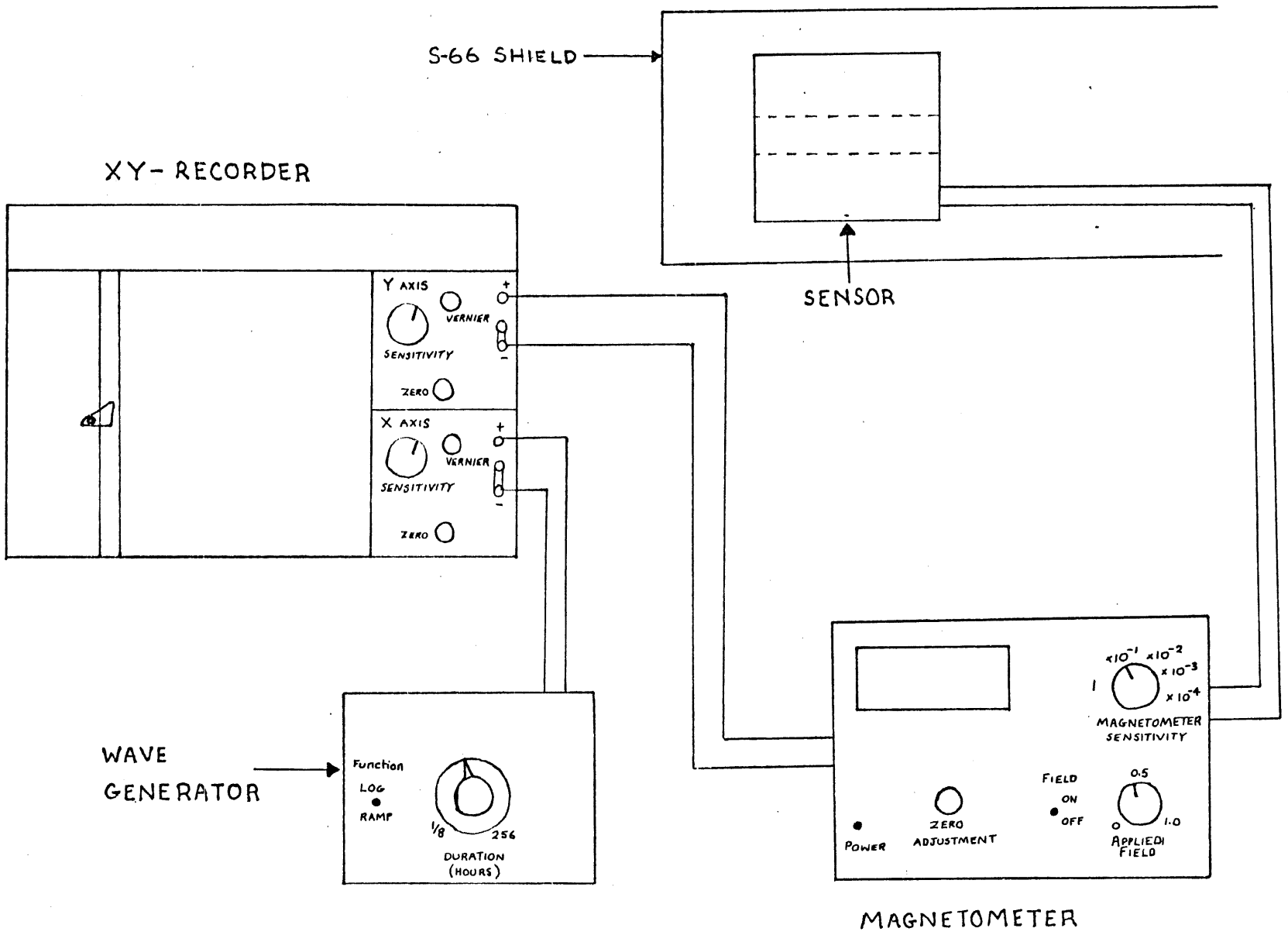
S-66 SHIELD
SENSOR
XY- RECORDER
Y AXIS
VERNIER
SENSITIVITY
ZERO
X AXIS
VERNIER
SENSITIVITY
ZERO
WAVE
GENERATOR
Function
LOG
RAMP
1/8
256
DURATION
(HOURS)
MAGNETOMETER
SENSITIVITY
POWER
ZERO
ADJUSTMENT
FIELD
ON
OFF
0.5
0
1.0
APPLIED
FIELD
MAGNETOMETER

FIGURE 1

1 millivolt/inch, plus a vernier which can be calibrated for intermediate scales.

The maximum output from the magnetometer is ±2V. The maximum deflection of the Y axis is 7" but this can be extended by offsetting the zero adjustment.

iii) Wave generator - The wave generator is made by the Schonstedt Instrument Company and is connected to the X axis of the XY recorder. The wave generator can provide either a ramp or log function with a range of sweep times from 1/8 hour to 256 hours. The ramp function provides a linear increase with time and was used for most experiments. The log function provides a logarithmic increase with time but due to the malfunction of the instrument calibration of the log time base was rather difficult.

For operating and set-up instructions including zero adjustments see appendix A.

Experimental procedure

A sample is selected and placed in the plastic cubic holder. This cubic holder is then placed into the oblong wooden chuck. The wooden chuck is then slid into the square cavity of the sensor which is inside the shield. The remanent magnetization of the sample is now indicated on the digital display, and recorded on the XY recorder.

To start the experiment the applied field is then switched on as is the wave generator. The value which is now indicated on the magnetometer display is the summation of three quantities (see Figure 2 below). It is the initial remanence plus the magnitude of the applied field, H, plus the induced magnetization.

Figure 2.

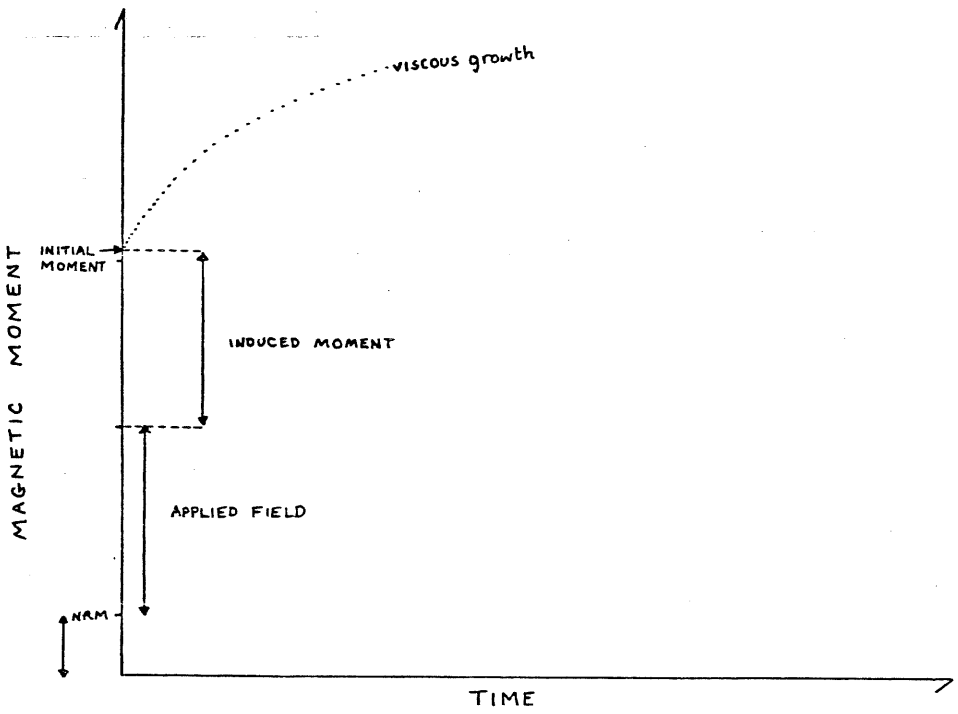

Any subsequent change in this value is then recorded as a viscous remanent magnetization.

N.B. It is important to note that the magnetometer measures the magnetic field only in the long direction of the Chuck i.e. along the axis of the coil. This is also the direction in which the field is applied. Hence the NRM measured is a component of the true NRM in the axial direction.

Experimental Problems

As mentioned before the maximum output of the magnetometer was ± 2 volts, above this the readout on the magnetometer goes off scale. This was a major drawback because the sensitivity of the instrument was restricted to $x10^{-1}$ emu/V or lower when applied fields of 0.3 oe or more were used.

e.g. For an applied field of 1.0 oe ≃ 0.079 emu

on $x10^{-1}$ emu/V sensitivity 1.0 oe produces 0.7 volts

on $x10^{-2}$ emu/V sensitivity 1.0 oe produces 7.0 volts

i.e. off scale

A high sensitivity was needed because the change in magnetization of the sample (VRM) was small compared to the induced magnetization, usually by a factor of 20 or more. To overcome this problem of reduced magnetometer sensitivity, the sensitivity of the XY-recorder had to be increased. However similar problems arose here with

keeping the recorder on scale.

e.g. Applied field = 1.0 oe (≃ 0.0079 emu)

J_i (induced magnetization) = 0.1287 emu

maximum possible sensitivity = $x10^{-1}$ emu/V, hence the maximum output from the magnetometer is 1.287 volts

XY recorder deflection	scale	
1.287 in	1V/in	
12.87 in	100mV/in	
128.7 in	10mV/in	i.e. off scale

Inorder to obtain a measurable VRM component the 10mV/in scale must be used, however under these conditions the induced magnetization sends the XY-recorder off scale (maximum deflection is 7 in.).

To solve this problem a simple modification was made to the equipment (see Figure 3).

Figure 3.

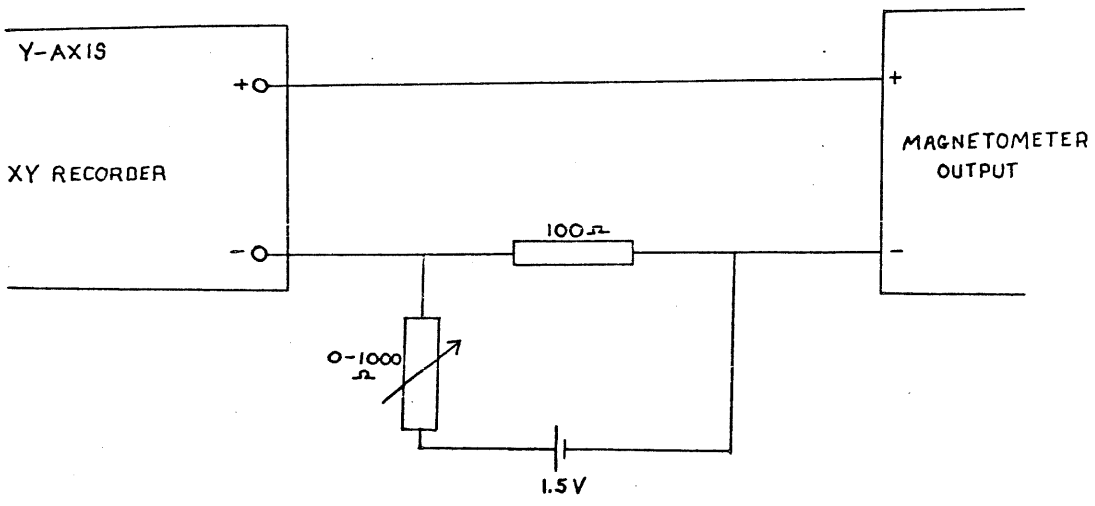

A 1.5 Volt dry cell and a potential divider circuit was used as illustrated above to produce an emf equal and opposite to the magnetometer output, hence reducing the voltage across the XY-recorder terminals to zero. This circuit allows the 10mV/in sensitivity on the XY-recorder to be used. In practice 4 dry cells were connected in parallel to minimize the current drain and to prolong battery life.

For small applied fields i.e. 0.1 oe to 0.2 oe the sensitivity of the magnetometer is not restricted to the lower ranges. In this case the above modification does not have to be used, instead the zero adjustment on the magnetometer is offset according to the expected induced magnetization.

Results

Not all the experiments performed produced useful data and only about 10 experiments were suitable for actual mathematical calculation of parameters.

The growth curves obtained were categorized into quality grades A, B, and C on the basis of two things. One was the magnitude of the VRM, the other was the smoothness and regularity of the growth curves.

Table 1 shows the grade A experiments run along with the sample number, applied field strength, length of experiment, and comments on

each growth cruve. Tables 2 and 3 show similar information for grade B and C experiments respectively.

Looking at the grade A curves first (see Figures 4 and 5) we see that the growth curves show smooth, even growth with very minor fluctuations compared to the actual growth. These curves are typical of the grade A type curves.

N.B. Figures 4 to 9 are actual data. It was deemed necessary to include actual data because any reproduction would have resulted in loss of accuracy.

Looking at Figure 4 for example, one can see that the initial magnetization is 1.323×10^{-1} emu and that the magnetization grows with time, until after 16 hours the magnetization is 1.355×10^{-1} emu. This change in magnetization with time in an applied field is the VRM growth.

These grade A growth curves have a rapid increase in magnetization to begin with but gradually decreases to a stable plateau. It is this curve from which produces a straight line (linear relationship) when the VRM is plotted against the logarithm of time.

Grade B growth curves are not as simple as grade A curves and commonly show two forms. One type is where there is a distinct step in the growth curve e.g. Figure 6, as though one growth was superimposed on another. The other type is where there is a growth curve

TABLE 1 Grade A

Sample #	Experiment run	Applied Field H (oe)	Length of run (hrs)	Comments on the growth curve	J_v vs logt plot Figure No.
20.24	33	0.1	16	Smooth even growth curve but on a small scale.	12
423.36	38	1.0	16	Large +ve smooth growth curve but not levelling off enough.	10
423.36	39	DECAY CURVE	2.5	Decay curve of expt. 38, smooth and even but short time span.	10
423.36	27	0.1	16	Large -ve growth curve with minor irregularities.	10
538.26	40	1.0	16	Large +ve, smooth growth, slightly uneven near the end.	11
538.26	41	DECAY CURVE	8	Decay curve of expt. 40, fairly smooth with slight variations.	11
861.15	42	1.0	16	Large +ve smooth growth, very small variations.	12
861.15	29	0.1	16	Large +ve growth with minor variations.	12

TABLE 2 Grade B

Sample #	Experiment Run	Applied Field H (oe)	Length of Run (hrs)	Comments on the growth curve
20.24	48	1.0	4	Large +ve rapid growth but went offscale in 5 hrs.
173.14	10	0.1	8	Large -ve growth but there is a step at 7 hrs.
201.05	11	0.1	16	Large +ve growth with a distinct step in the growth at 5 hrs.
382.67	18	0.1	16	Large +ve growth with a definite step in the growth at 6 hrs.
382.67	25	0.1	16	Large -ve growth but with a distinct step around 9 hrs.
423.36	35	1.0	16	Smooth +ve growth but on a small scale.
538.26	26	0.1	8	Smooth growth -ve but with a definite break in slope at $\sim$ 7 hrs.
538.26	36	1.0	64	Smooth +ve growth but on a small scale.
861.15	46	0.5	2	Small +ve growth over a short time span.
BDA 26-5-12	20	0.1	6.5	-ve growth with variations

TABLE 3 Grade C

Sample #	Experiment Run	Applied Field H (oe)	Length of Run (hrs)	Comments on the growth curves
20.24	22	0.1	4	First a rapid decrease then a slow increase over a period of 4 hrs.
173.41	8	0.1	16	Small +ve growth at first then a decrease near the end of the run.
173.62	14	0.1	16	Small +ve growth then a decrease at the end of the run.
173.62	31	0.1	8	No growth just variations about the induced moment.
204.88	34	0.1	7	Little growth very noisy.
204.88	43	1.0	16	Small increase then a decrease around 9 hrs. followed by a rapid increase which tapers off.
204.88	45	1.0	16	Moderate +ve growth but very variable.
BDA 107-4-4	17	0.2	4	No growth very variable.
107-4-5	23	0.1	16	No growth very variable.
107-4-5	44	1.0	128	Very variable, +ve growth after an initial decrease.
107-4-7	16	0.1	64	Variable with a rapid increase, stabilization then rapid decrease to initial value.
107-4-7	24	0.1	8	No growth very variable.
26-5-12	28	0.1	8	Smooth, variable small increase
26-5-12	30	0.1	64	No growth very variable.

but the variability about the mean value is greater than for grade A curves (see Figure 7).

Grade C curves are those which showed little or no relationship between VRM and time. In general grade C curves showed very small growth with alot of irregularity (see Figures 8 and 9).

From the grade A and B growth curves data could be extracted to test the relationship between VRM and the logarithm of time.

From Néel's theory (1950, 1955) which was derived earlier in equation (11):

$$J_v(t_a,H) + J_i(H) = pS_vH(\log t_a - \log t_o) + (P/2)H^2$$

where

$$\log(t_a/t_o) \ll H/S_v$$

In the Rayleigh region i.e. small fields $J_i \alpha H^2$ hence

$$(13) \quad J_v(t_a,H) = J_i(H) + S_a(\log t_a - \log t_o)$$

This equation can be simplified to the equation of a straight line:

$$(14) \quad J_{VRM} = J_{INDUCED} + S_a(\log t_a)$$

where

J_{VRM} is the viscous remanent magnetization

$J_{INDUCED}$ is the induced remanent magnetization

S_a is the viscosity coefficient

t_a is the acquisition time.

The logarithm of the acquisition (or decay) time was plotted versus the viscous remanent magnetization. From these plots the viscosity coefficient can be calculated. It is simply the slope of the line. The viscosity coefficients are recorded in table 4.

Looking at the grade A VRM vs logt plots (Figures 10 to 12), one finds a generally linear relationship with only slight variations away from a straight line, e.g. experiment runs 42, 41, 39, 29, and 27. Run 33 (Figure 12) shows more variability about the straight line but this is within the error for this run because of the small scale used. Run 40 (Figure 11) shows a linear increase for the first 10 hours after which there is a temporary decrease in slope before resuming its initial slope. Run 38 (Figure 10) increases linearly for the first 8 hours after which the slope increases until about 14 hours when the slope approximates the original slope again. The deviation of the plots away from the straight line fit near the beginning is seen in most cases. This effect has been reported by other authors as well (Lowrie, 1974).

If we now look at the grade B plots (Figures 13 to 16) a different situation is found. There is no longer the simple linear relationship betwen VRM and logt. Most grade B growth curves show a multistage growth in which there is a step or change in slope e.g. experiment runs

TABLE 4

sle # (depth) m	Experiment Run	S_a (viscosity coefficient) emu/gm/oe x 10^5	Grade	Rock type Basalt
IRDP 20.24	33	9.9 ± 2.0	A	dyke
20.24	48	8.9 ± 5.0	B	dyke
IRDP 173.14	10	3.6 ± 2.5	B	flow
173.41	8	4.3 ± 2.5	B	flow
IRDP 201.05	11	5.2 ± 2.5	B	flow
IRDP 382.67	25	8.6 ± 2.5	B	flow
382.67	18	14.0 ± 2.5	B	flow
IRDP 423.36	38	5.0 ± 2.5	A	dyke
423.36	35	7.5 ±10	B	dyke
423.36	27	13.3 ± 2	A	dyke
423.36	39	4.9 ± 2.5	A	dyke
IRDP 538.26	40	6.7 ± 2.5	A	dyke
538.26	36	6.5 ±10	B	dyke
538.26	41	4.8 ± 2.5	A	dyke
538.26	26	6.6 ± 2.5	B	dyke
IRDP 861.15	42	4.6 ± 2.5	A	flow
861.15	29	15.9 ± 2.5	A	flow
861.15	46	1.9 ± 2.5	B	flow
BDA 26-5-12	20	4.7 ± 2.5	B	oceanic submarine

26, 25, 18 and 11. Some plots simply have only a few data points e.g. experiment runs 48 and 46, (Figure 13) however they do approximate straight lines. Experiment run 36 (Figure 13) shows a linear relationship for the first 16 hours after which the slope increases almost exponentially. The signal to noise ratio is generally higher for grade B curves when compared to grade A curves (e.g. compare Figure 4 and 7).

The viscosity coefficients, (S_a) which are calculated from the slope of the J_v vs logt plots are first normalized for sample weight and then scaled for the magnitude of the applied field (i.e. divide S_a by WH, where W is the sample weight and H is the applied field in oersteds). The resultant values are recorded in table 4. The coefficients vary between 3.6 and 15.9 x 10^{-5} emu gm^{-1} oe^{-1} and the errors shown in table 4 are the errors determined from the growth curve (i.e. the variability about an average growth line). If the average viscosity coefficient is calculated for dykes and flows, we find that the dyke average of 7.5 x10^{-5} emu gm^{-1} oe^{-1} is very close to the flow average of 7.3 x 10^{-5} emu gm^{-1} oe^{-1} (i.e. within the experimental error of $\pm$2.5 x 10^{-5} emu gm^{-1} oe^{-1}).

In two cases, acquisition experiments were run back to back with decay experiments (i.e. both the acquisition and decay of VRM was recorded), e.g. experiment runs 38 and 39, and 40 and 41.

The viscosity coefficients of acquisition and decay for the above runs (see Table 4) are equal to each other within the experimental error

ranges, e.g.

for sample 423.36 $S_a = 5.0 \times 10^{-5} \pm 2.5 \times 10^{-5}$ emu gm^{-1} oe^{-1}

$S_d = 4.9 \times 10^{-5} \pm 2.5 \times 10^{-5}$ eum gm^{-1} oe^{-1}

the difference is 2%

for sample 538.26 $S_a = 6.7 \times 10^{-5} \pm 2.5 \times 10^{-5}$ emu gm^{-1} oe^{-1}

$S_d = 4.8 \times 10^{-5} \pm 2.5 \times 10^{-5}$ emu gm^{-1} oe^{-1}

the difference is 29%

The conclusion is that there is no significant difference within experimental uncertainties.

If we now consider the Bermudan rocks, out of the four samples studied (BDA 107-4-4, 107-4-5, 107-4-7, 26-5-12) only 26-5-12 showed a linear relationship between the VRM and $\log t_a$ (see Figure 14). The growth curves for unit 107 were mostly grade C showing no measurable growth, (see Figure 8 and 9 and Table 3).

Discussion of Results

We have seen that the grade A J_v vs logt plots generally produce straight lines (i.e. there is a direct relationship between J_v and logt). There are exceptions to this rule; some curves show a definite change in slope, e.g. run 38, figure 10. These changes seem to be temporary though, because the slope seems to come back to its initial value.

Grade B curves show most definite steps in their growth curves. These steps produce distinct increases in the slopes of the J_v vs logt plots, although after this abrupt increase the slope returns to its

initial slope approximately. This change also seems to occur around the same time (1 to 2 x 10^{-4} secs). This change in slope has been observed by other authors (Creer, 1970; Kent and Lowrie, 1977; Dunlop and Hale, 1976). There is no adequate explanation of this phenomena in the literature. Dunlop (1973c) suggested that this non-linearity may be due to an irregular grain distribution.

The non-linearity found in this study may be due to the equipment though. For example if there were fluctuations in the mains supply this might affect the applied field. A sudden surge in the power supply may increase the field producing a second VRM growth superimposed on the first. A way of checking this would be to monitor the mains supply while an experiment was being run.

If we now look at the viscosity coefficients we find that they are comparable (i.e. within each other's error) for sample numbers 20.24, 173.14 and 173.41, 538.26, and just about comparable for sample number 382.67 (see table 4). However there are two samples (sample numbers 423.36 and 861.15) which have experimental runs (27 and 29) giving coefficients much higher than the others calculated for those samples. These values coincide with applied fields of 0.1 oe compared to 1.0 oe for the other experimental runs performed on these samples. However run 26 for sample number 538.26 was run in a 0.1 oe field and its' coefficient is comparable to the other runs of 538.26.

The only explanation I would suggest is that these values are due to experimental error. More experiments would have to be done to determine whether or not these anomalous values are real.

FIG 4

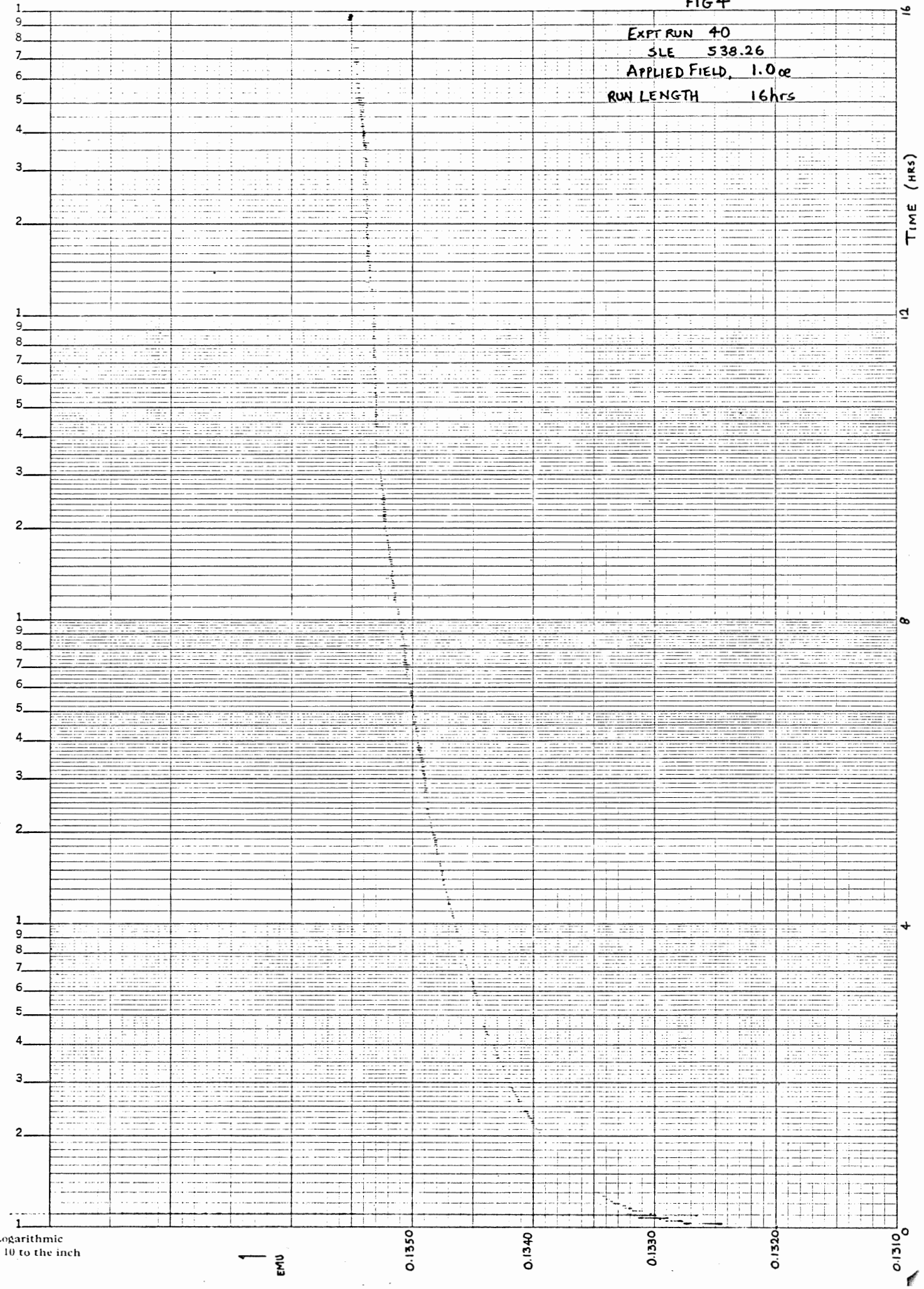
EXPT RUN 40
SLE 538.26
APPLIED FIELD, 1.0 oe
RUN LENGTH 16 hrs
TIME (HRS)
16
12
8
4
0
0.1350
0.1340
0.1330
0.1320
0.1310
EMU
Semi-Logarithmic
4 Cycles x 10 to the inch

FIG. 5

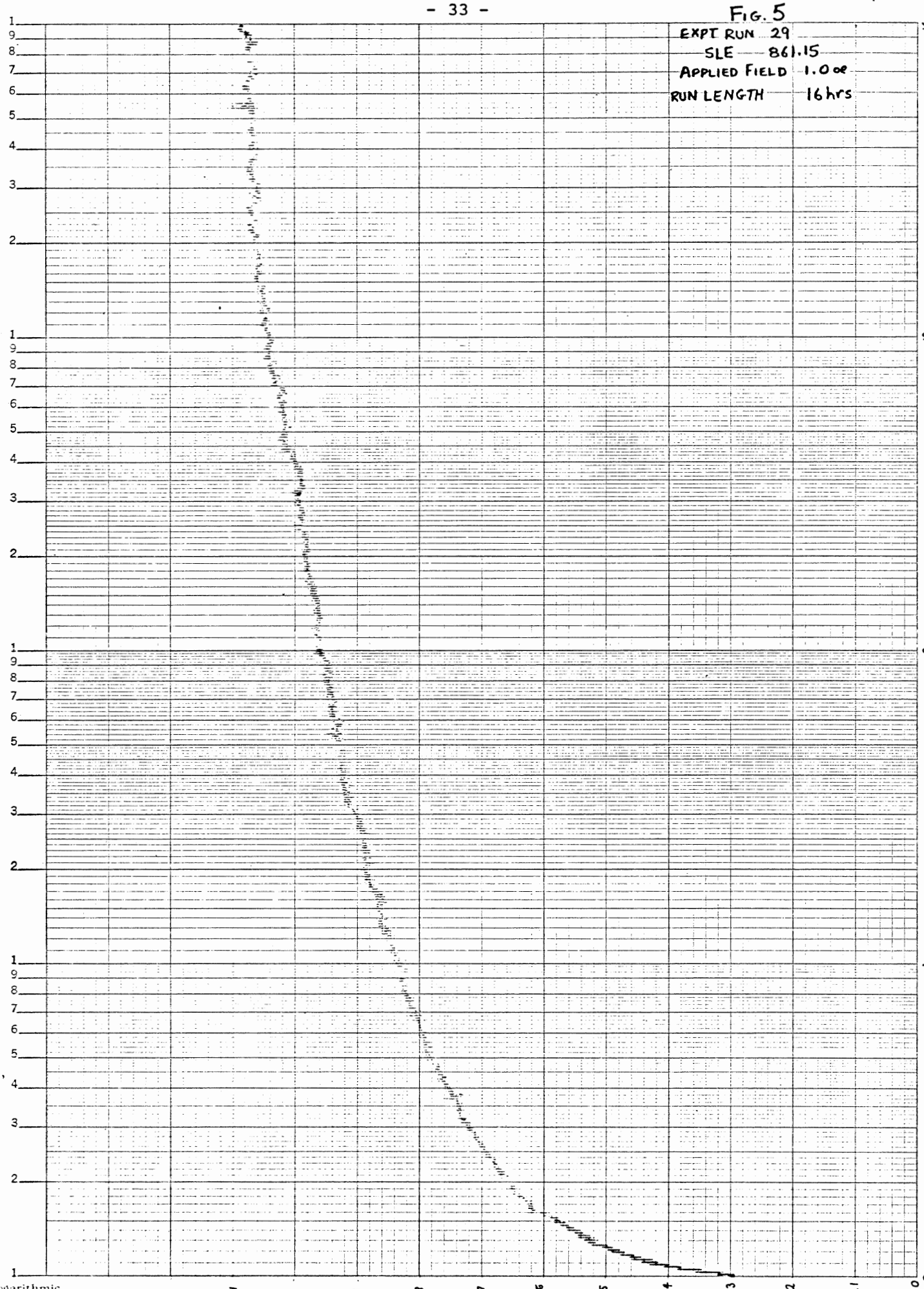

Semi-Logarithmic
4 Cycles x 10 to the inch

FIG. 6

EXPT RUN 18
SLE 382.67
APPLIED FIELD 0.1oe
RUN LENGTH 16 hrs

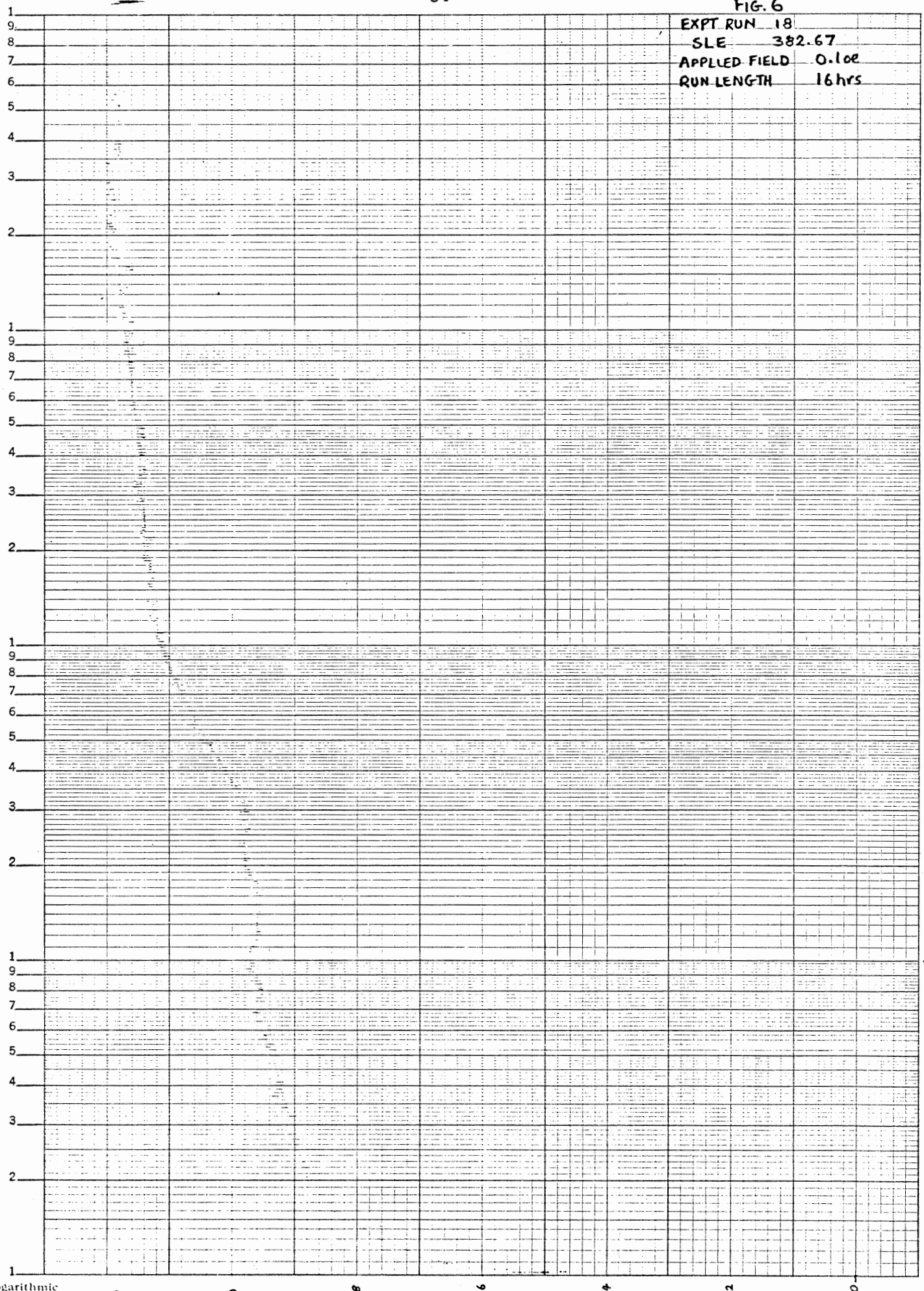

Semi-Logarithmic
4 Cycles x 10 to the inch

Fig.7

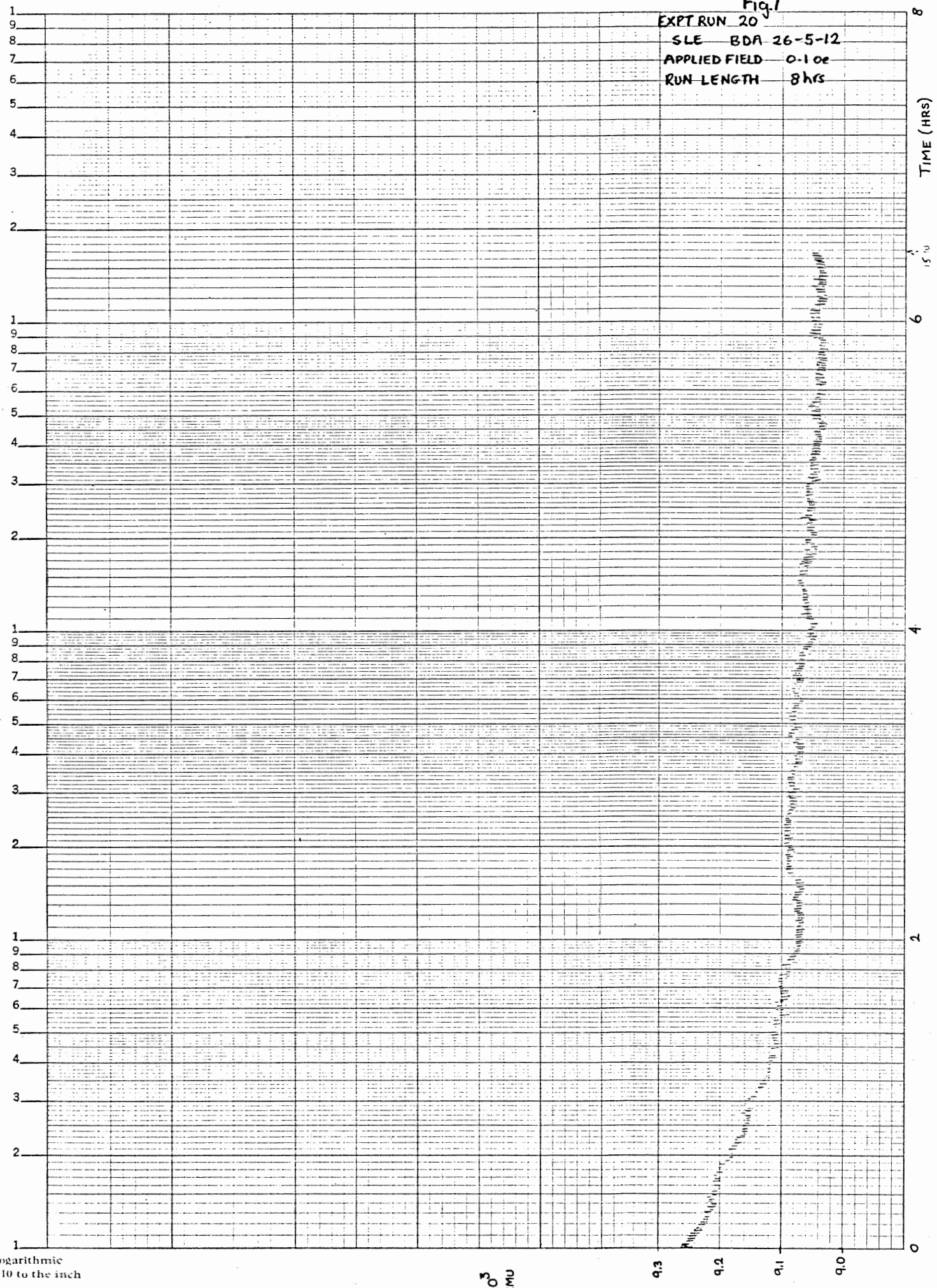

Semi-Logarithmic
4 Cycles x 10 to the inch

FIG. 8

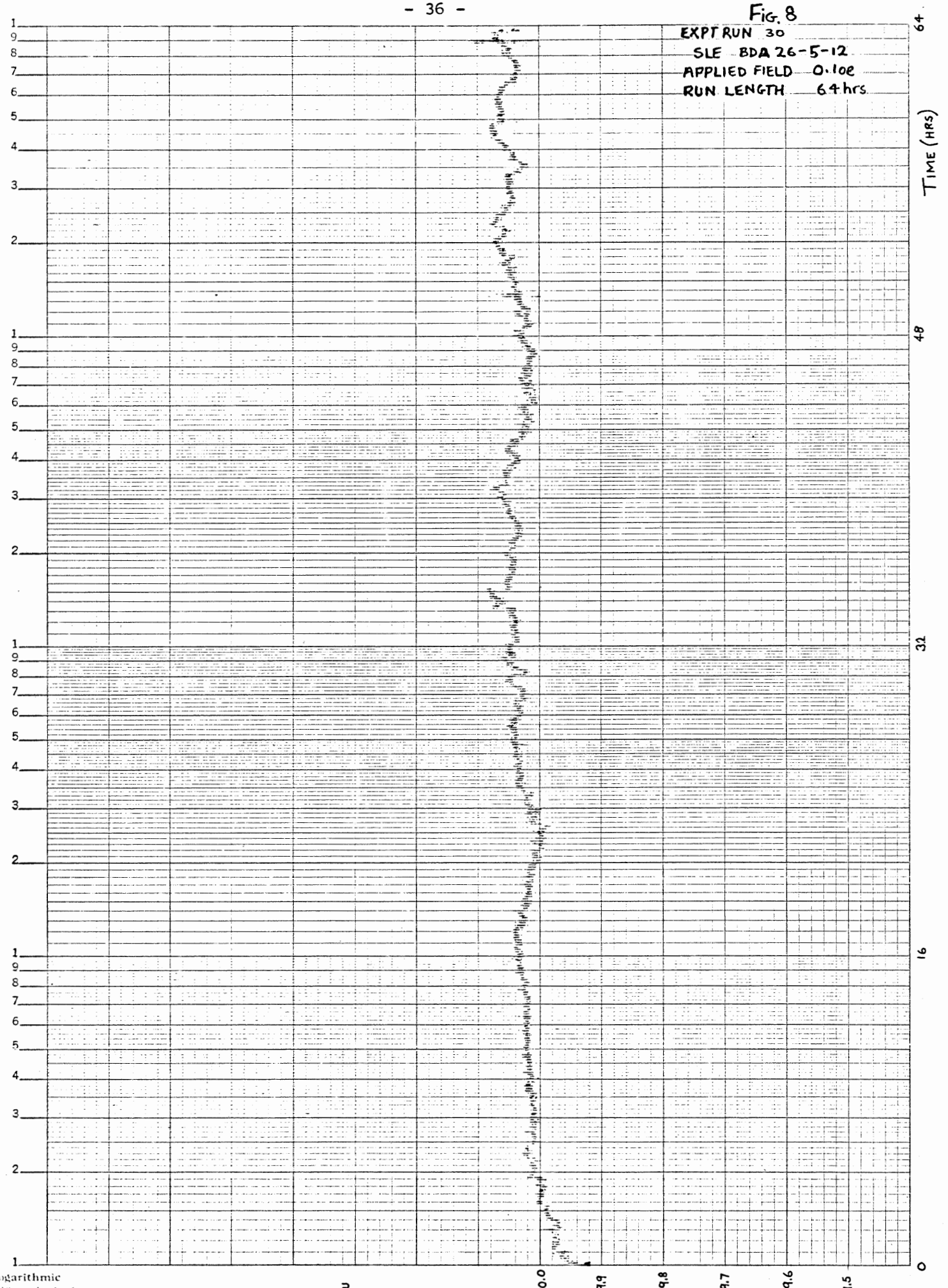

Semi-Logarithmic
4 Cycles x 10 to the inch

FIG. 9

EXPT RUN 23
SLE BDA 107-4-5
APPLIED FIELD 0.1 OE
RUN LENGTH 16 hrs

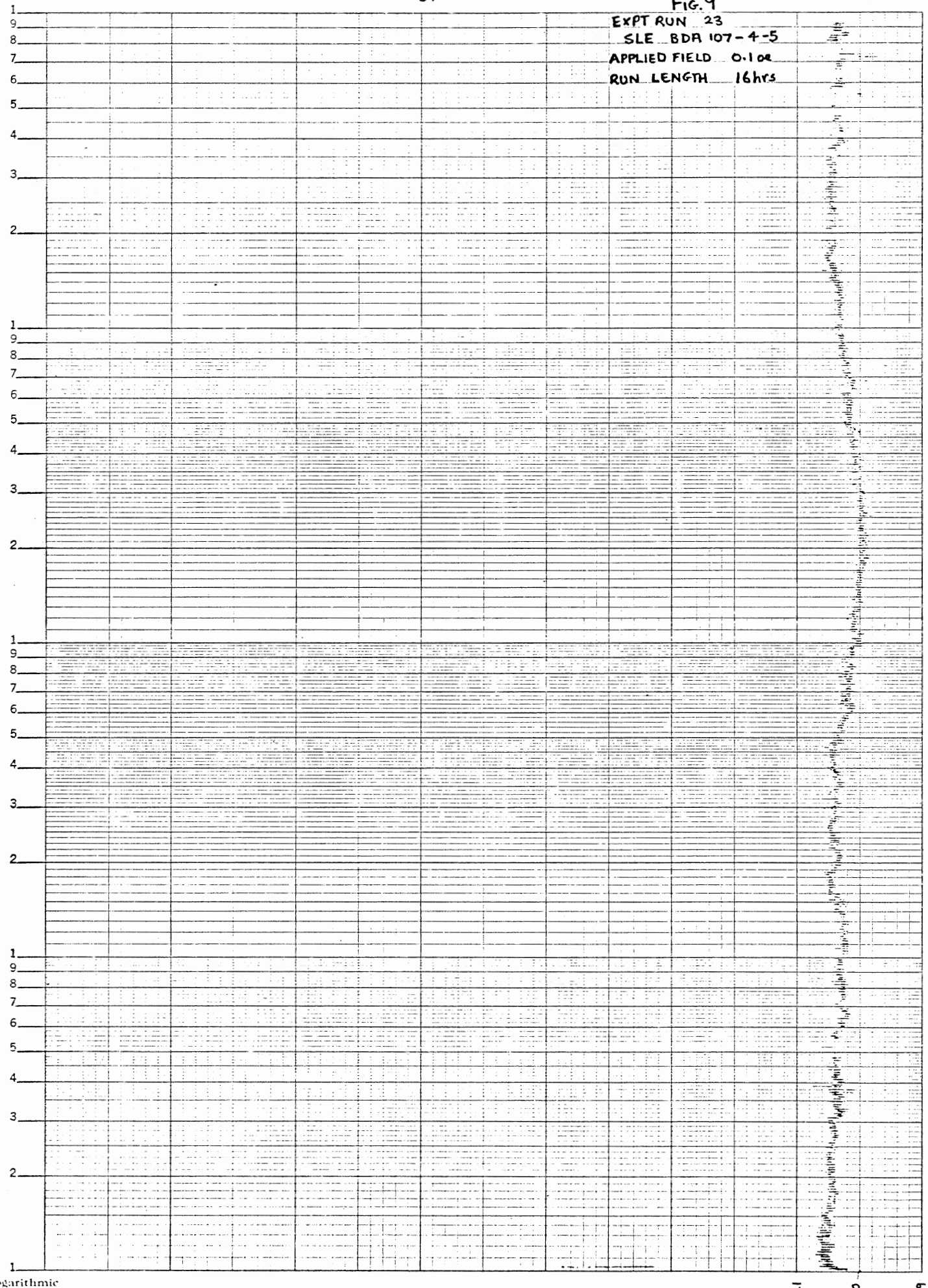

Semi-Logarithmic
4 Cycles x 10 to the inch

FIGURE 10

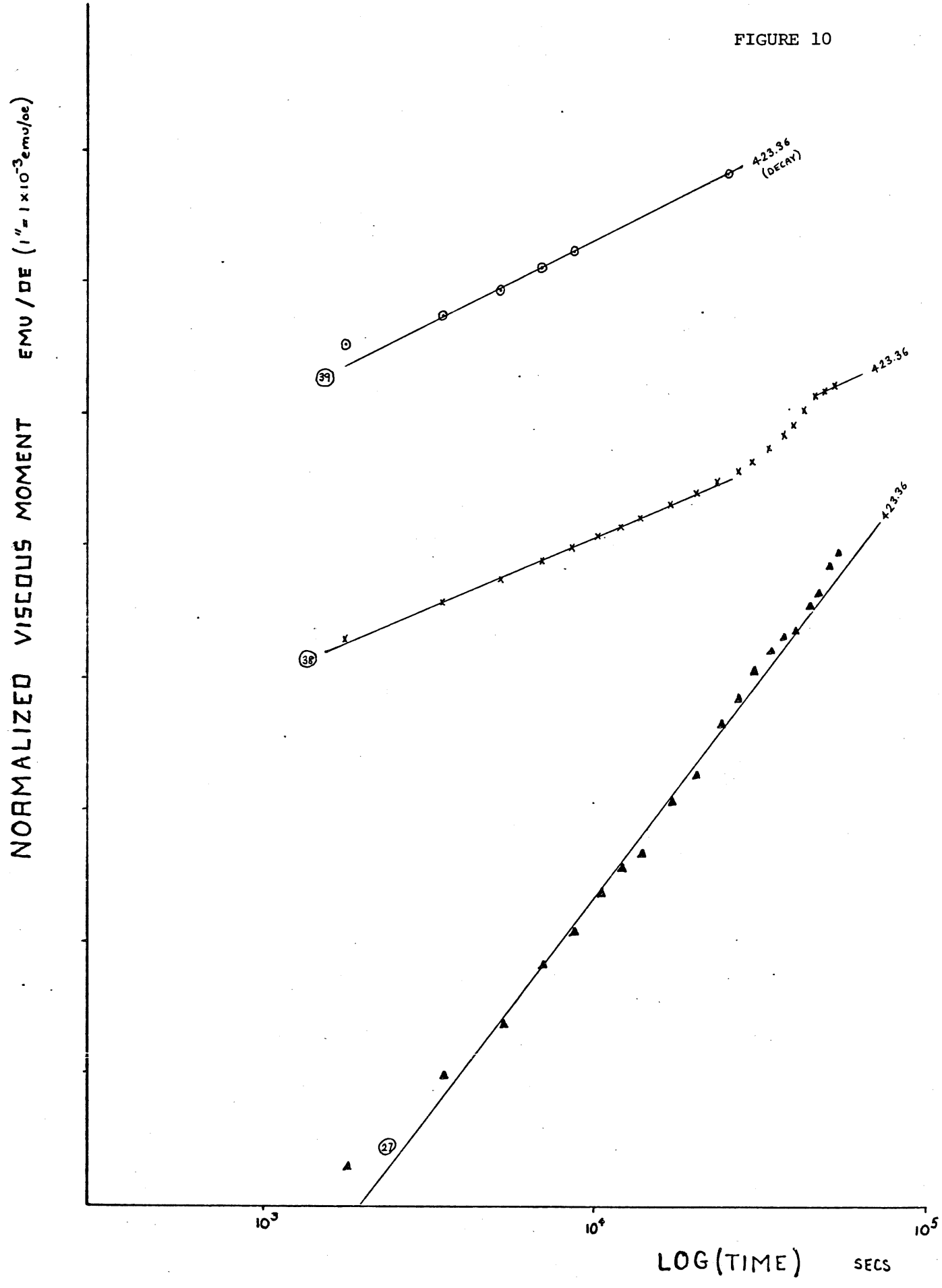
NORMALIZED VISCOUS MOMENT EMU/OE (1" = 1 x 10⁻³ emu/oe)
423.36 (DECAY)
423.36
423.36
39
38
27
10³
10⁴
10⁵
LOG (TIME) SECS

FIGURE 11

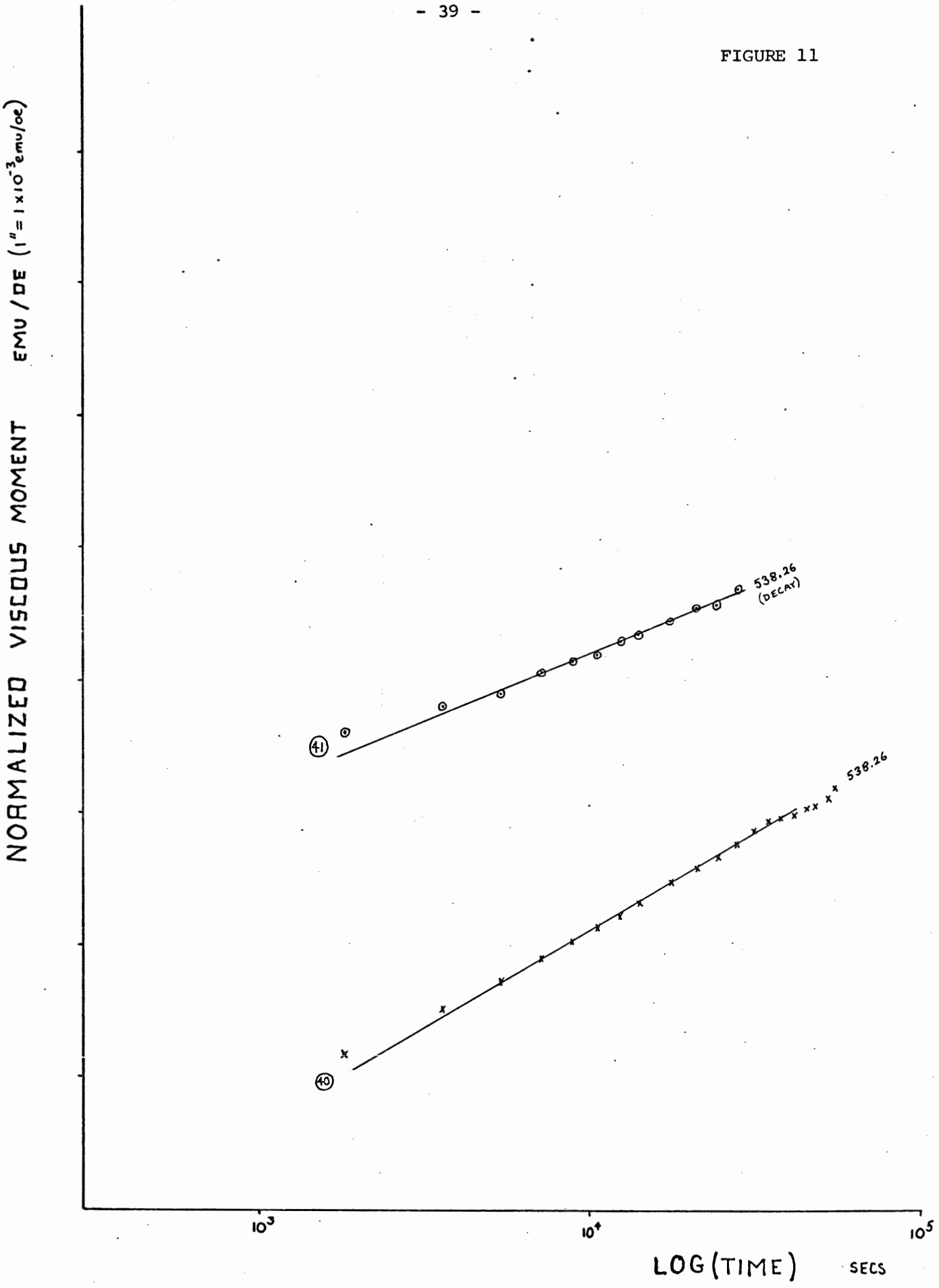
NORMALIZED VISCOUS MOMENT EMU/OE (1" = 1 x 10⁻³ emu/oe)
538.26 (DECAY)
41
538.26
40
10³
10⁴
10⁵
LOG (TIME) SECS

FIGURE 12

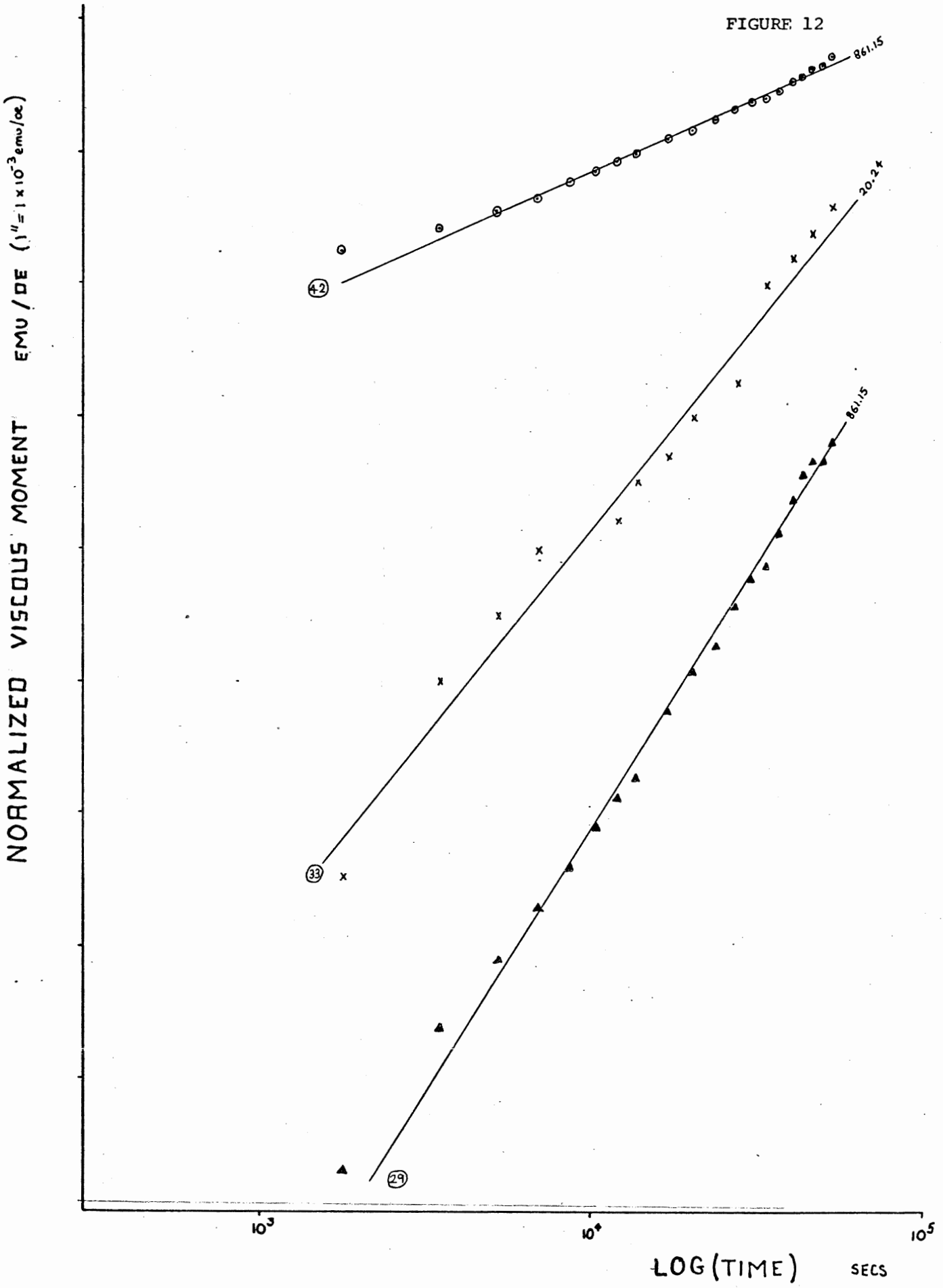
NORMALIZED VISCOUS MOMENT EMU/OE (1" = 1 x 10⁻³ emu/oe)
861.15
4-2
20.2K
33
861.15
29
10³
10⁴
10⁵
LOG (TIME) SECS

FIGURE 13

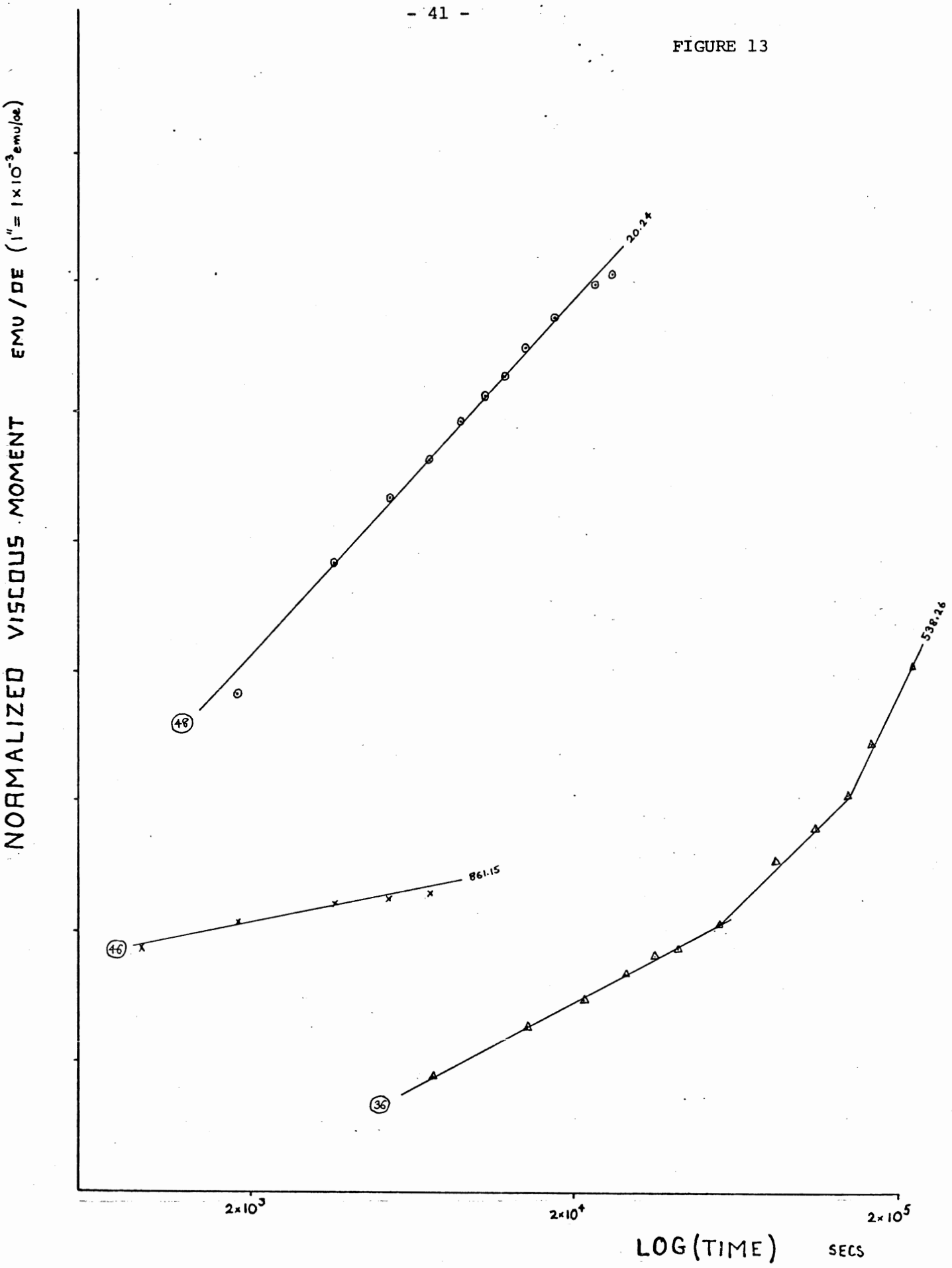
NORMALIZED VISCOUS MOMENT EMU/OE (1" = 1×10⁻³ emu/oe)
20.24
538.26
861.15
48
46
36
2×10³
2×10⁴
2×10⁵
LOG (TIME) SECS

FIGURE 14

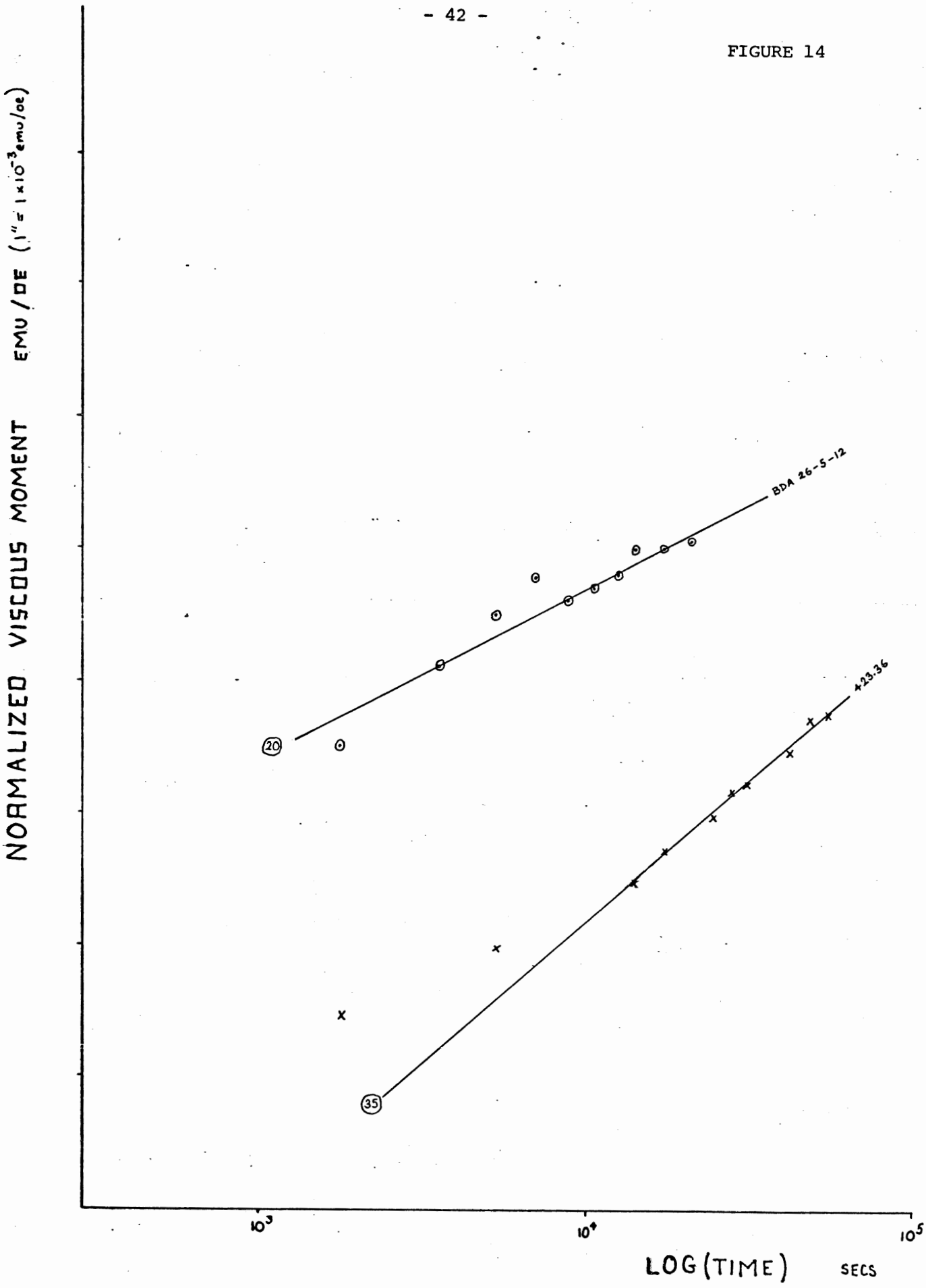
NORMALIZED VISCOUS MOMENT EMU/OE (1" = 1×10⁻³ emu/oe)
BDA 26-5-12
20
4-23.36
35
10³
10⁴
10⁵
LOG (TIME) SECS

FIGURE 15

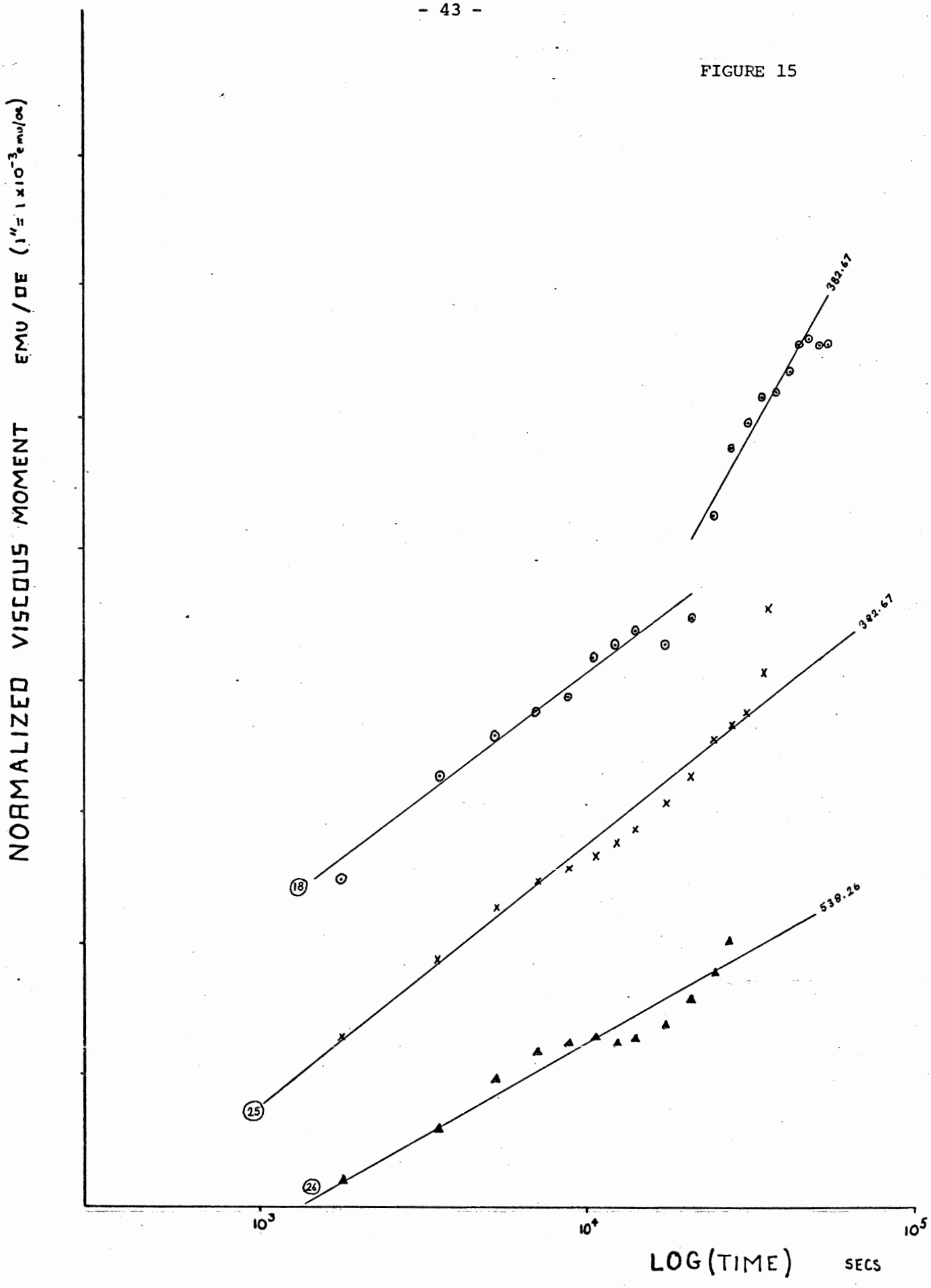
NORMALIZED VISCOUS MOMENT EMU/OE (1"= 1 x 10⁻³ emu/oe)
382.67
382.67
538.26
18
25
24
10³
10⁴
10⁵
LOG (TIME) SECS

FIGURE 16

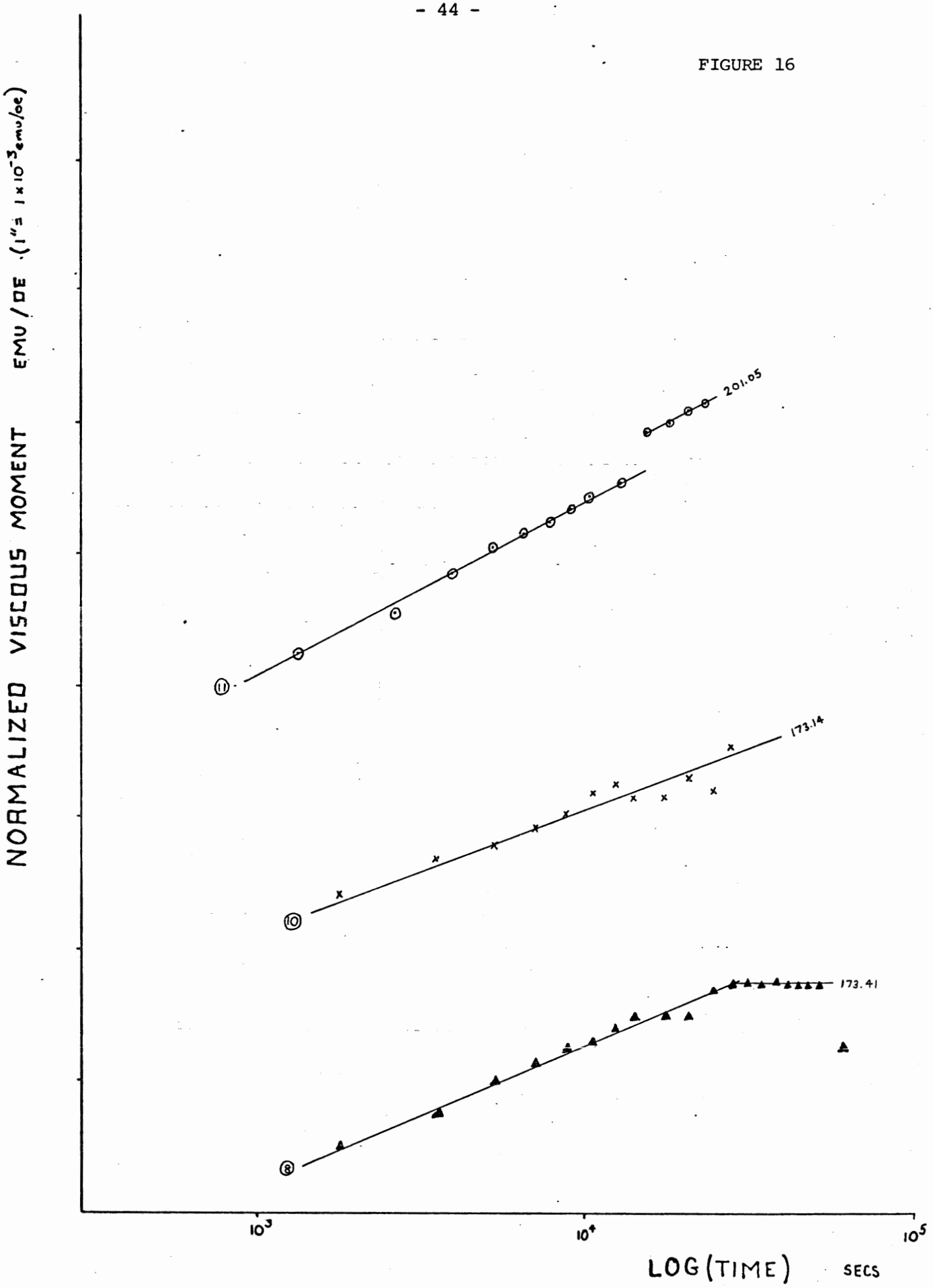
NORMALIZED VISCOUS MOMENT EMU/OE (1" = 1×10⁻³ emu/oe)
201.05
173.14
173.41
11
10
8
10³
10⁴
10⁵
LOG (TIME) SECS

Susceptibility

This magnetic parameter is easily measured on this VRM system and is simply the ratio of the induced magnetization to the applied field:

$$k = \frac{J_i}{H \text{ applied}}$$

To demonstrate this direct relationship two short experiments were performed in which the induced moment was recorded for different applied fields, see Figures 17 and 18.

The susceptibility of all the samples used have been tabulated in Table 5.

This method of measuring susceptibility is certainly fast but how accurate it is remains to be determined. Perhaps measurements of susceptibility can be made by another technique e.g. by an AC bridge to see if the results are comparable or by using a standard for which the susceptibility is known.

N.B. It is difficult to measure J_i for some samples which acquire VRM rapidly, i.e. to separate J_i from J_v.

The differences in susceptibility measurements for 15.95, 20.24 and 173.62 are due to this rapid increase in VRM (see Table 5).

FIGURE 17

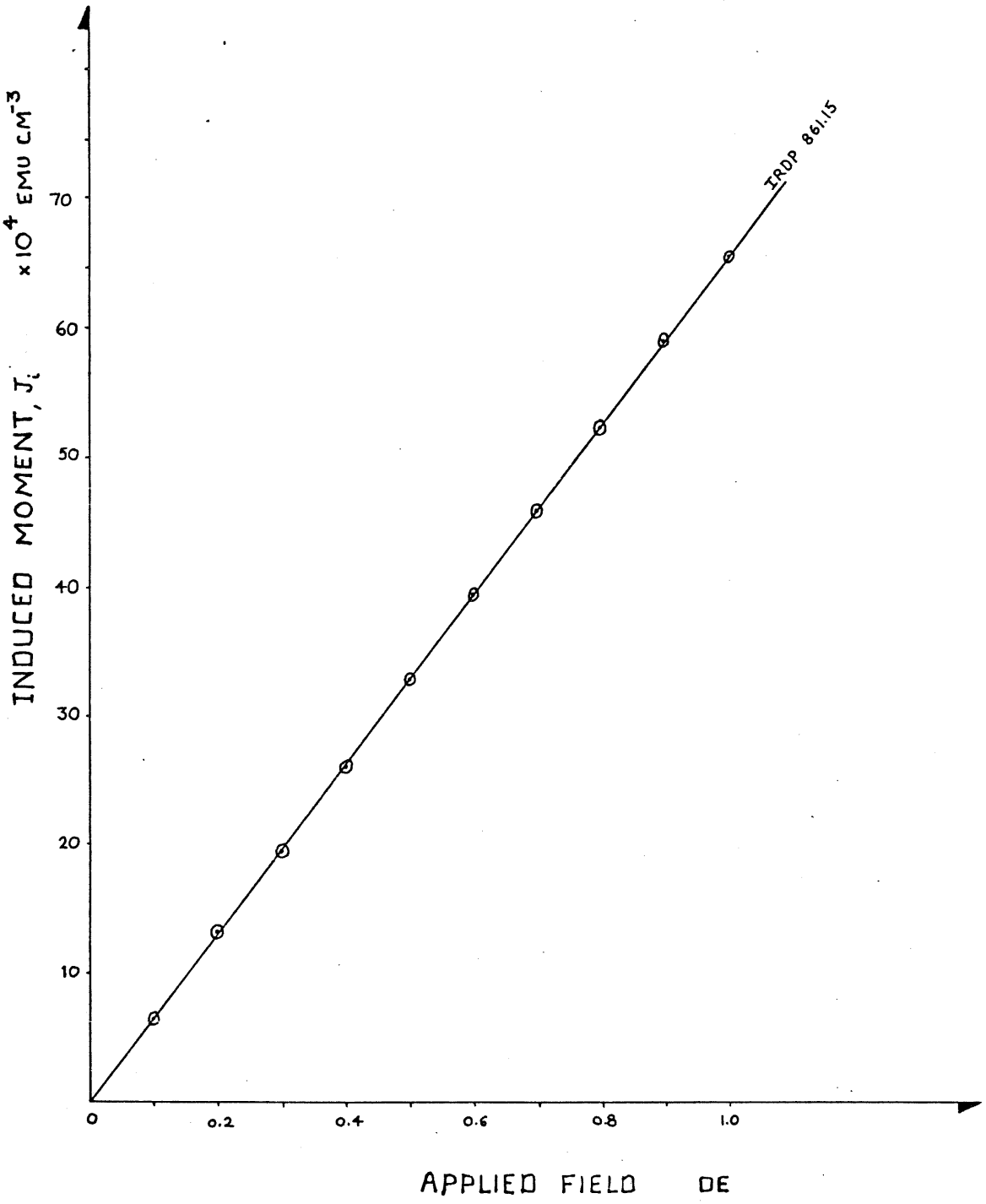
INDUCED MOMENT, J_i $\times 10^4$ EMU CM^{-3}
70
60
50
40
30
20
10
0
0.2
0.4
0.6
0.8
1.0
APPLIED FIELD DE
IRDP 861.15

FIGURE 18

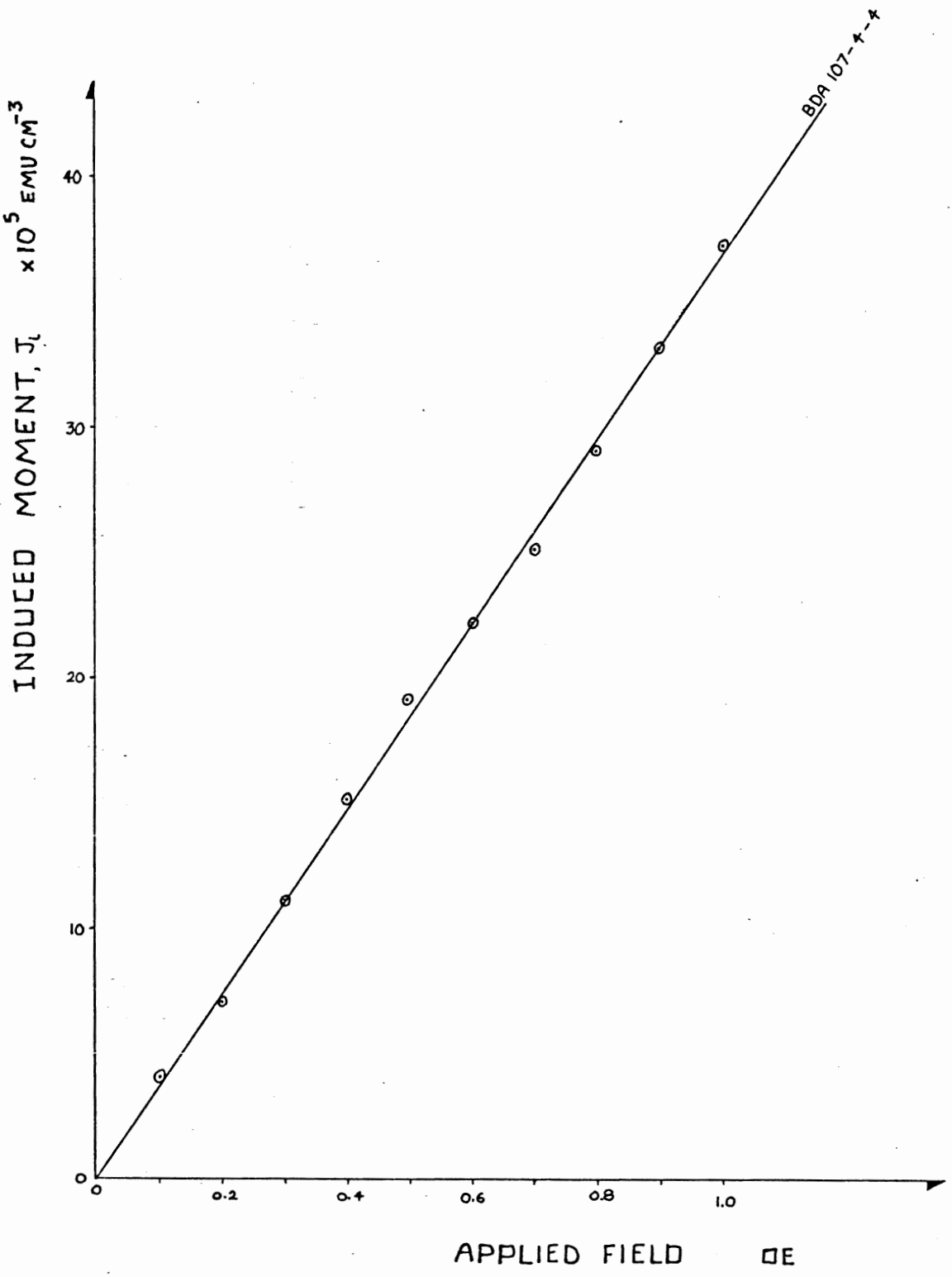
INDUCED MOMENT, J_i $\times 10^5$ EMU CM^{-3}
BDA 107-4-4
0
10
20
30
40
0
0.2
0.4
0.6
0.8
1.0
APPLIED FIELD ΩE

TABLE 5 Susceptibility Measurements

Sle #	Susceptibility $k \times 10^{6}$ emu cm^{-3} oe^{-1}		H oe
IRDP 15.95	5842		0.1
	3455		1.0
20.24	3405		1.0
	5382		0.1
24.245	4356	3876 ± 480	0.1
	3396		1.0
47.85	4797	4828 ± 31	0.1
	4859		1.0
173.14	7471		0.1
	7535	7521 ± 43	0.5
	7556		1.0
173.41	6904	6899 ± 6	0.1
	6893		1.0
173.62	5335		0.1
	7479		1.0
201.05	4416	4453 ± 37	0.1
	4490		1.0
204.88	2194		0.1
382.67	8423	8474 ± 51	0.1
	8524		1.0
423.36	9134		0.1
	7894	8311 ± 413	0.5
	7904		1.0
538.26	7647	7687 ± 40	0.1
	7727		1.0
861.15	6566		graph
BDA 107-4-5	183	216 ± 33	0.1
	248		1.0
107-4-7	96	135 ± 39	0.1
	173		1.0
107-4-4	367		graph
26-5-12	1768		0.1

Conclusions

In evaluating the performance of the VRM apparatus several minor problems arose but in general the equipment produced some good results (depending on the samples as well). The circuit modification, see Figure 3, although simple allows the complete range of applied fields to be used in conjunction with the greatest possible sensitivity on the XY-recorder. However the sensitivity of the magnetometer is still restricted to $x10^{-1}$ emu/V for applied fields over 0.2 oe. This is offset though by the fact that increased magnetometer sensitivity would mean more 'noise'.

Among the recommendations to be made a safety device to prevent the XY-recorder from going off scale would definitely be an asset. Another recommendation is to arrange for a chart recorder to monitor the mains supply fluctuations and to see if it has any effect on the experiments (especially non-linearity).

In general the IRDP rocks showed a linear relationship between VRM growth and the logarithm of time. There are some cases where non-linear behaviour was observed especially when one looks at the grade B curves (i.e. distinct steps in the growth). This non-linearity is either due to the magnetic properties of the rock or because of experimental conditions. The viscosity coefficients (see Table 4) are in general agreement within the experimental error. These are exceptions though (runs 27 and 29); these anomalous values may be due to

experimental conditions because they were from some of the earlier experiments. Stricter and constant experimental conditions would be a way of determining whether the non-linear growth and anomalous viscosity coefficients were real effects or not.

From Tables 1, 2 and 3 it is indicated whether the growth curves show an increase or decrease (i.e. a positive or negative acquisition). Some samples seem to show a decrease from the initial induced moment (analogous to a decay), see Figure 7, although the samples were being exposed to an applied field. All the samples with negative acquisition curves were run in applied fields of 0.1 oe after having been exposed to the Earth's field (0.5 oe). There are two possible interpretations:

1) The VRM is acquired in an apposite direction to the NRM effectively reducing the NRM.
2) This negative acquisition is actually a decay curve because the applied field is smaller than the ambient field to which the sample was exposed.

In order to make sure that a viscous growth (positive acquisition) is observed I recommend that samples be allowed to decay in zero field for approximately 24 hours before conducting any VRM experiment especially when small fields are being

Actual decay experiments run produce coefficients which are approximately equal (i.e. within experimental error limits) to their

respective acquisition coefficients.

There appears to be no significant difference between basaltic flows or diabase dykes as far as the viscosity coefficients are concerned.

The experiments carried out on the Bermudan samples was not successful in obtaining any quantitative data, except for BDA 26-5-12. The irregularity of the VRM records (see Figures 8 and 9) run on unit 107 suggest that either viscous growth is naturally complex of that exposure to the Earth's geomagnetic field has already produced a VRM. The recent history of these samples is unknown and so precludes any statement that can be made about them.

The susceptibility measurements made were quick and easy and are shown in Table 5. The susceptibility for the IRDP rocks show values from 30 x 10^{-4} emu cm^{-3} oe^{-1} to 90 x 10^{-4} emu cm^{-3} oe^{-1} which is about average for subaerial basalts (Telford, 1977). The Bermudian susceptibilities are quite low in comparison 1-2 x10^{4} emu cm^{-3} oe^{-1} for unit 107. This indicates that the Bermudan rocks are 'less magnetic' than the IRDP rocks.

References

Barbier, J.-C. 1951. Jour. Phys. Radium, 12, pp. 352-354.

Barbier, J.-C. 1953. Thesis, University of Grenoble, France.

Biquand, D. and Prevot, M. 1971. Zeits. fur Geophysik, 37, pp. 471-485.

Briden, J.C. 1965. Jour. Geophys. Research, 77, pp. 5205-5221.

Creer, K. M. 1957. Phil. Trans. Roy. Soc. Lond. Ser. A, 250, pp. 130-143.

Creer, K. M., Petersen, N., and Petherbridge, J. 1970. Geophys. Jour. Roy. Astro. Soc., 21, pp. 471-483.

Davison, G. 1979. Honours Thesis, Dalhousie University.

Dunlop, D. 1973c. Rev. of Geophys. and Space Phys., 11, pp. 855-901.

Dunlop, D. and Hale, C. J. 1977. Can. J. Earth Sci., 14, pp. 716-739.

Ewing, J. A. 1885. Phil. Trans. Roy. Soc. Lond., 176, pp. 523-650.

Kawai, N. and Kume, S. 1953. J. Geomagn. Geoelect., 5, pp. 66-70.

Kawai, N. and Kume, S. 1959. Jour. Phys. Radium, 20, pp. 258-261.

Kent, D. V., Lowrie, W. 1978. Jour. Geophys., 44, pp. 297.

LeBorgne, E. 1960. Ann. Geophys., 16, pp. 445-494.

Lowrie, W. 1974. Jour. of Geophys., 40, pp. 513-536.

Néel, L. 1949. Ann. de Géophy., 5, pp. 99-136.

Néel, L. 1950. Jour. Phys. Radium, 11, pp. 49-61.

Néel, L. 1955. Advan. Phys., 4, pp. 191-243.

Pechnikov, V. S. 1967. Izv. Akad. Nauk SSSR, Ser Fiz.Zemli, 6, pp. 134-136.

Preisach, F. 1935. Z. Phys., 94, pp. 277-302.

Rice, P. H. 1978. M.Sc. Thesis, Dalhousie University.

Richter, G. 1937. Ann. Physik, 29, pp. 605-637.

Rimbert, F. 1959. Rev. Inst. Franc. Pétrole, XIV, pp. 1-123.

Shimizu, Y. 1960. Jour. Geomagn. Geoelect., 11, pp. 125-138.

Sholpo, L. E. 1967. Izv. Earth Phys., 6, pp. 99-116.

Stacey, F. D. 1963. Advanc. Phys., 12, pp. 45-133.

Street, R. and Wooley, J. C. 1949. Proc. Phys. Soc. Lond. Sect. A, 62, pp. 562-572.

Street, R. et al. 1952. Proc. Phys. Soc. Lond. Sect. B., 65, pp. 679-696.

Telford Geldart Sherrif Keys, Applied Geophysics, 1977.

Thellier, E. 1938. Ann. Inst. Phys. Globe Univ. Paris Bur. Cent. Magn. Terr., 16, pp. 157-302.

Trukhin, V. I. 1966. Izv. Earth Phys., 2, pp. 105-111.

Yakubailik, E. K. 1968. Izv. Akad. Nauk SSSR, Ser Fiz. Zemli, 10, pp. 104-106.

Zhilyaeva, V. and Kolesnikov, L. 1966. Izv. Earth Phys., 2, pp. 738-743.

APPENDIX A

SET-UP INSTRUCTIONS

for

SVM-1

1. Demagnetize S-66 Shield.
2. Put the sensor unit in the shield and wedge in place so sensor is snug enough not to move when inserting sample holder; front of sensor should be ≃ 13" from the front opening of the shield.
3. Plug sensor unit into back of electronics unit.
4. Hook up 115 power and turn the instrument ON. It should warm up for at least 10-15 minutes before starting the adjustments.
5. Use the NEUTRALIZING control to obtain a meter reading of less than ± 0.100 with the multiplier switch set at 1×10^{-2}.
6. Set APPLIED FIELD switch in "O" position, set METER MULTIPLIER at 1×10^{-2}. Turn the APPLIED FIELD switch ON and OFF (on is up) and note if meter reading changes, if it does adjust FIELD ZERO (screwdriver adjustment on front panel). If meter reading is high reduce with NEUTRALIZING control. Switch MULTIPLIER to 1×10^{-3} and recheck field zero adjustment. Return MULTIPLIER to 1×10^{-2}.
7. Turn APPLIED FIELD switch OFF. Set the APPLIED FIELD switch at the 1 oerstedt position. Turn the APPLIED FIELD switch ON and OFF and note any change in reading on the meter. Adjust for no change with the FIELD BALANCE potentiometer (screwdriver adjustment on the front panel). If the adjustment is beyond range of the potentiometer, center the potentiometer adjustment (≃ 12 turns from either end as it is a 25 turn potentiometer) and adjust the

mechanical position of the sensor unit in the shield to bring the difference to within approximately .100 on the 1 x 10^{-2} scale, then secure the sensor position and make the final adjustment with the potentiometer.

8. Interconnect the SVM-1 and the sweep generator with an X-Y recorder. The recorder output on the back of the SVM-1 (Red and Black terminals) should be connected to the Y-Axis input of the recorder and the sweep generator is connected to the X-Axis of the recorder. Sensitivity of the recorder output for the various switch positions is 1 Volt for the EMU value shown on the meter multiplier except for the maximum clockwise position of the multiplier switch. This position provides meter sensitivity the same as the proceeding position but increases recorder output sensitivity to 1 Volt/1 x 10^{-4} EMU. (Note: In this position the recorder output will reach the ± 2 Volt limit at meter reading of ± 0.200). Normally, the SVM-1 sensitivity is set at the highest value that will keep the meter and the recorder output "ON-SCALE" for the specimens being measured. The zero adjustment and sensitivity of the plotter Y-Axis are set based on the expected voltage change at the recorded output terminals.

9. To set the X-Axis recorder controls, turn on the power switch on the sweep generator. Turn the RUN-RESET switch to RESET and the LOG-RAMP switch to RAMP. Use the recorder X zero adjustment to set the pen at the center of the paper. Then turn the LOG-RAMP to the LOG position and adjust the X-Axis recorder sensitivity to position

the pen at the left paper margin. Recheck the zero adjustment in the RAMP position and the gain control in the LOG position, as these adjustments may interact. If the log sweep is to be used, leave the adjustment obtained above. If a linear (RAMP) sweep is to be used, leave the sensitivity adjustment obtained above, turn the switch to RAMP and readjust the recorder X zero adjustment to move the pen to the left edge of the paper.

OPERATING INSTRUCTIONS

for

SVM-1

1. Turn the SVM-1, the sweep generator and the X-Y recorder on and let warm up for 10 to 15 minutes.
2. On the SVM-1, turn the FIELD CONTROL "OFF", and set the METER MULTIPLIER and APPLIED FIELD switches to the desired positions.
3. On the Sweep Generator, set the RUN-RESET switch in the RESET position, select either LOG or RAMP operation and set the SWEEP DURATION switch at the desired position.
4. Install the specimen in the cubic sample holder and place the sample holder in the chuck. Note that the measurement direction is parallel to the long dimension of the chuck and that magnetization directed toward the front of the chuck (toward the open end of the shield) produces a positive output on the meter and a positive voltage at the recorder output connections. The applied field is also directed toward the open end of the shield so that susceptibility and viscous change are always in the positive direction.

   It may be desirable to install a group of samples in sample holders and store them on the bottom of the shield in front of the SVM-1 Sensor Assembly to let any existing viscous component decay. They can be transferred to the chuck without exposure to Earth's Field.

5. Place the chuck and sample on the bottom of the shield and adjust the NEUTRALIZING control for a zero reading on the meter and drop the pen on the X-Y recorders.
6. Gently slide the chuck into the cavity in the sensor unit. The meter will now indicate the remanent magnetization of the specimen. You can mark the position on the X-Y plotter by moving the X zero adjustment.
7. If you are making a linear time plot of magnetization vs time turn the sweep generator switch to RUN then turn the SVM-1 Field control "ON". For a long plot operate both switches simultaneously. The early part of the log plot will be quite ragged as the log function is developed from a linear staircase function and the first few steps are quite large.
8. The magnitude of the step in output, beginning at the remanent value, corresponds to the susceptibility of the specimen divided by the magnitude of the applied field.
9. You will have to record starting time to determine completion time as there is no "End of Sweep" indicator. At the end of the sweep the sweep generator will hold until manually reset.
10. By lifting the recorder pen, resetting the sweep generator, lowering the recorder pen and restarting the sweep generator at the same time, you turn the applied field off, you can record the viscous decay of the sample.
11. Always turn the APPLIED FIELD switch OFF when inserting or removing samples to avoid accidental exposure to the field (when inserting the next sample).